



Machine-learning strategies in laser-plasma physics

Andreas Döpp^{1,2,3}, Faran Irshad¹, Sunny Howard^{1,3}, Jannik Esslinger¹, Nils Weisse¹,
Christoph Eberle¹, Jinpu Lin¹, Robin Wang³, Peter Norreys³, Stefan Karsch^{1,2}

¹ Centre for Advanced Laser Applications, Faculty of Physics, LMU Munich

² Max Planck Institute for Quantum Optics (MPQ)

³ Faculty of Physics, Oxford University



Team DOLPHIN

Data-driven Optimization of Laser Physics and Interactions



PhD students

Sunny Howard

Jannik Esslinger

Chris Eberle

Jakob Schröder

Collaborators in CALA

Stefan Karsch

Faran Irshad

Nils Weisse

Jinpu Lin

Collaborators in Oxford

Peter Norreys

Robin Wang



Machine learning in laser-plasma physics



- Held **1st online workshop on control systems and machine learning** in January 2022 (150+ registered participants)
- **Special issue** in High-Power Laser Science and Engineering.
- Pre-print of **review paper** (30+ pages) **recently published on arXiv**

arXiv:submit/4626985 [physics.plasm-ph] 30 Nov 2022

Data-driven Science and Machine Learning Methods in Laser-Plasma Physics

Andreas Döpp,^{1,*} Christoph Eberle,¹ Sunny Howard,^{1,2} Faran Irshad,¹ Jinpu Lin,¹ and Matthew Streeter³

¹Ludwig-Maximilians-Universität München, Am Coulombwall 1, 85748 Garching, Germany

²Department of Physics, Clarendon Laboratory, University of Oxford, Parks Road, Oxford OX1 3PU, United Kingdom

³Centre for Plasma Physics, Queens University Belfast, Belfast BT7 1NN, United Kingdom

Laser-plasma physics has developed rapidly over the past few decades as lasers have become both more powerful and more widely available. Early experimental and numerical research in this field was dominated by single-shot experiments with limited parameter exploration. However, recent technological improvements make it possible to gather data for hundreds or thousands of different settings in both experiments and simulations. This has sparked interest in using advanced techniques from mathematics, statistics and computer science to deal with, and benefit from, big data. At the same time, sophisticated modeling techniques also provide new ways for researchers to deal effectively with situation where still only sparse data are available. This paper aims to present an overview of relevant machine learning methods with focus on applicability to laser-plasma physics and its important sub-fields of laser-plasma acceleration and inertial confinement fusion.

CONTENTS

I. Introduction	2	C. Downhill simplex method and gradient-based algorithms	22
A. Laser-Plasma Physics	2	D. Genetic algorithms	23
B. Why data-driven techniques?	3	E. Bayesian optimization	23
II. Modeling & prediction	4	F. Reinforcement learning	26
A. Predictive models	4	V. Unsupervised Learning	27
1. Spline Interpolation	5	A. Clustering	27
2. Regression	5	1. Centroid-based clustering	27
3. Probabilistic models	5	2. Distribution-based clustering	27
4. Gaussian process regression	6	B. Correlation analysis	27
5. Decision trees and forests	7	C. Dimensionality reduction	27
6. Neural networks	9	1. Principal component analysis	27
7. Physics-informed machine learning models	11	2. Autoencoders	28
B. Time series forecasting	12	VI. Image analysis	29
1. Classical models	12	A. Classification	29
2. State-Space Models	13	1. Support vector machines	29
3. Forecasting networks	13	2. Convolutional neural networks	29
C. Prediction and Feedback	14	B. Object detection	30
III. Inverse problems	15	C. Segmentation	31
A. Least squares solution	16	VII. Conclusions	31
B. Statistical inference	16	Acknowledgements	32
C. Regularization	16	References	32
D. Compressed sensing	17		
E. End-to-end deep learning methods	18		
F. Deep unrolling	19		
IV. Optimization	20		
A. General concepts	20		
1. Objective functions	20		
2. Pareto optimization	21		
B. Grid search and random search	22		

* a.doep@lmu.de

1. A. Döpp et al. **Data-driven Science and Machine Learning Methods in Laser-Plasma Physics**, *arXiv:2212.00026* (2022)

Machine learning in laser-plasma physics

- Held 1st online workshop on control systems and machine learning in January 2022 (150+ registered participants)
- **Special issue** in High-Power Laser Science and Engineering.
- Pre-print of review paper (30+ pages) recently published on arXiv (*accepted in High-Power Laser Science and Engineering*)

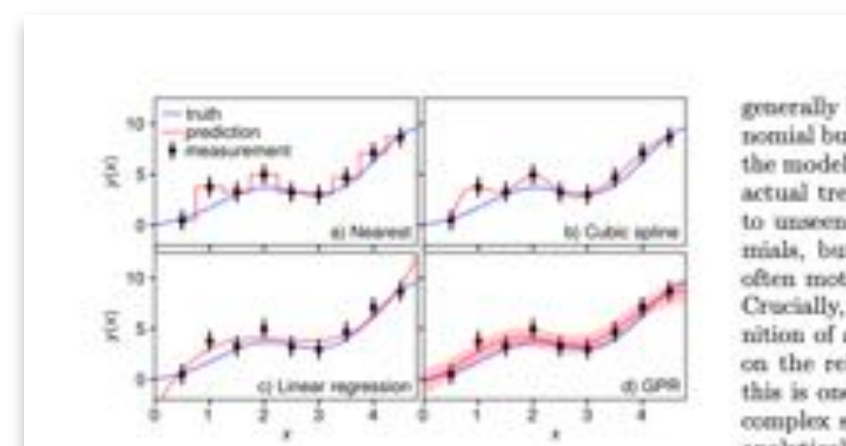


FIG. 2. Illustration of standard approaches to making predictive models in machine learning. The data was sampled from the function $y = x[1 + \sin x^2] + \epsilon$ with random Gaussian noise, ϵ , for which $\langle \epsilon^2 \rangle = 1$. The data has been fitted by a) nearest neighbour interpolation, b) cubic spline, c) linear regression, and d) Gaussian process regression.

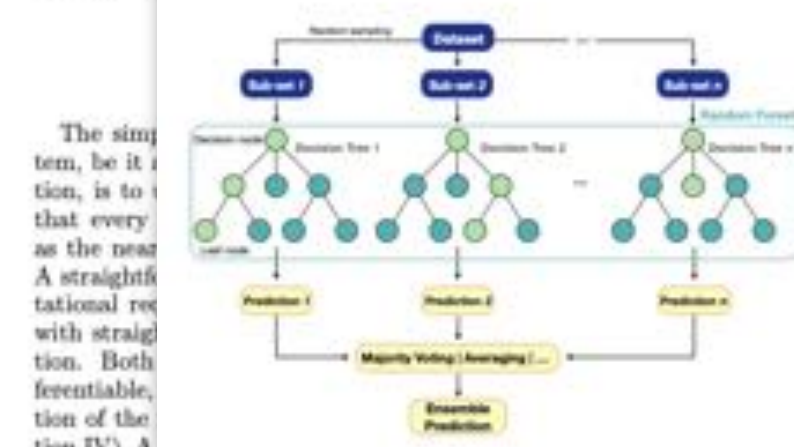


FIG. 4. Sketch of a random forest, an architecture for regression or classification consisting of multiple decision trees, whose individual predictions are combined using into an ensemble prediction e.g. via majority voting or averaging.

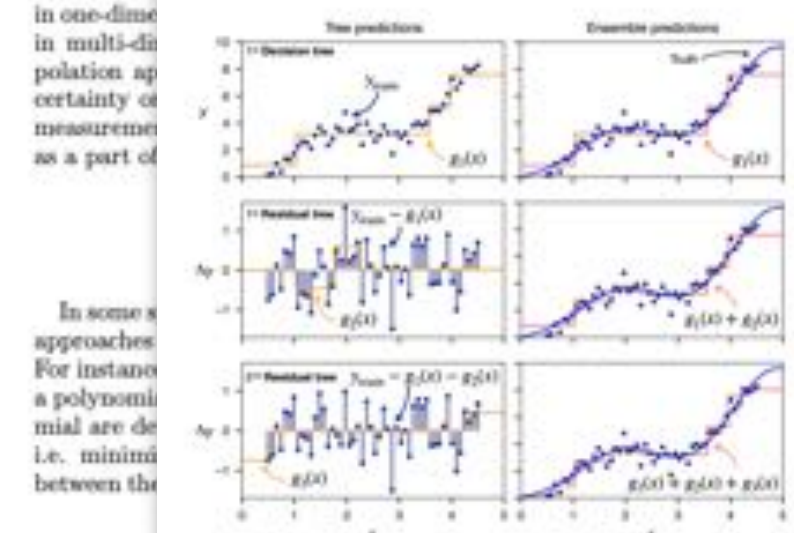


FIG. 5. Example of gradient boosting with decision trees. First, a decision tree g_1 is fitted to the data. In the next step, the residual difference between training data and the prediction of this tree is calculated and used to fit a second decision tree g_2 . This process is repeated n times, with each new tree g_n , learning to correct only the remaining difference to the training data. Data in this example sampled from same function as in Fig. 2 and each tree has a maximum depth of two decision layers.

In regression settings or entropy and information gain in a classification setting. At each decision point the data set is split and subsequently the metric is re-evaluated for the resulting groups, generating the next layer of decision nodes. This process is repeated until the leaves are reached. The more layers decision layers are used, called the depth of the tree, the more complex relationships can

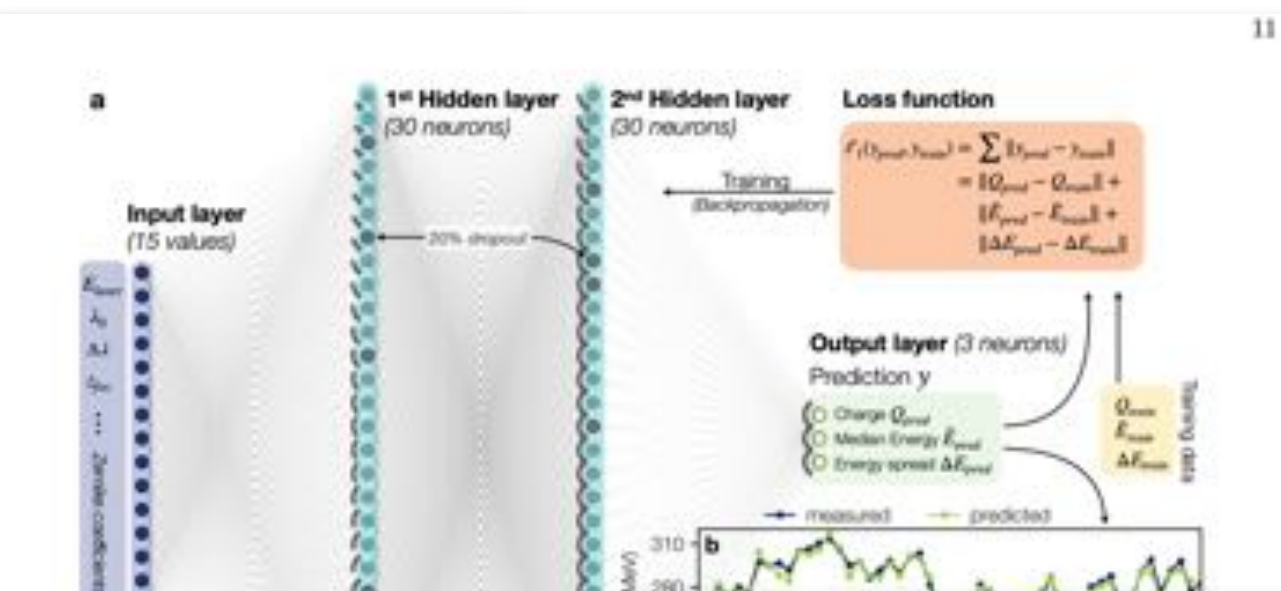


FIG. 7. Real-world example of a multilayer perceptron consists of 15 input neurons, two hidden layers with 30 neurons each and an output layer with 3 neurons. The input is derived from parasitic laser diagnostics (laser pulse energy E_p , longitudinal focus position x_{foc} and Zernike coefficients Z_n). 20% of neurons drop out for regularization during training. To evaluate the accuracy of the model, in this case using the median energy (E) and (c) measured and predicted energy E and ΔE adapted from Kirchen et al.²⁸

model incorporating a trained neural network was used to provide an additional computation package to the Geant4 particle physics platform. Neural networks are also trained to assist bohrraum design for ICF experiments by predicting the time evolution of the radiation temperature, in the recent work by McClaren et al.¹¹². In the work by Simpson et al.¹¹³, a fully-connected neural network with three hidden layers is constructed to assist the analysis of a x-ray spectrometer, which measures the x-rays driven by MeV electrons produced from high-power laser-solid interaction.

7. Physics-informed machine learning models

The ultimate application of machine learning for modeling physics systems would arguably be to create an "artificial intelligence physicist", as coined by Wu and Tegmark¹¹⁴. One prominent idea at the backbone of how to train a deep neural network. An example of using decision tree as an initializer are Deep Jointly-Informed Neural Networks (DJINN) developed by Humbird et al.⁹⁵, which have been widely applied in the high power laser community, especially in analyzing inertial confinement fusion datasets. The algorithm first constructs a tree or a random forest with tree depth set as a tunable hyperparameter. It then maps the tree to a neural network, or maps the forest to an ensemble of networks. The structure of the network (number of neurons and hidden layer, initial weights, etc.) reflects the structure of the tree. The neural network is then trained using back-propagation. The use of decision trees for initialization largely reduces the computational cost while maintaining comparable performance to optimized neural network architectures. The DJINN algorithm has been applied to several classification and regression tasks

Author, Year	Laser type	Optimization Method(s)	Free Parameters	Optimization goals
He et al., 2015 ¹⁰⁶	800 nm Ti:Sa, 15 mJ, 35 fs, 0.5 kHz	Genetic algorithm	deformable mirror (37 actuator voltages)	Electron angular profile, energy distribution & transverse emittance, optical pulse compression
Dann et al., 2015 ¹⁰⁷	800 nm Ti:Sa, 450 mJ, 40 fs, 5 Hz	Genetic & Nelder-Mead algorithms	deformable mirror or acousto-optic programmable dispersive filter	Electron beam charge, total charge within energy range, electron beam divergence
Shaloo et al., 2020 ¹⁰⁸	800 nm Ti:Sa, 0.245 J, 45 fs (bandwidth limit), 1 Hz	Bayesian optimization	Gas cell flow rate	Total electron beam energy, Electron charge within acceptance angle, Betatron X-ray counts
Jalas et al., 2021 ¹⁰⁹	800 nm Ti:Sa, 2.6 J, 39 fs, 1 Hz	Bayesian optimization	Gas cell flow rates (N_2); focus position and laser energy	Spectral charge density

TABLE I. Summary of a few representative papers on machine-learning-aided optimization in the context of laser-plasma acceleration and high-power laser experiments.

distributions, in this case the electron energy distribution. While simple at the first glance, these objectives need to be properly defined and there are often different ways to do so²⁰¹. In the example above, energy and bandwidth are examples for the central tendency and the statistical dispersion of the energy distribution, respectively. These can be measured using different metrics such as weighted arithmetic or truncated mean, the median, mode, percentiles and so forth for the former; and full width at half maximum, median absolute deviation, standard deviation, maximum deviation, etc. for the latter. Each of these seemingly similar measures emphasizes different features of the distribution they are calculated from, which can affect the outcome of optimization tasks. Sometimes one might also want to include higher order moments as objectives, such as the skewness, or use integrals, e.g. the total beam charge.

2. Pareto optimization

In practice, optimization problems often constitute multiple sometimes competing objectives g_i . As the objective function should only yield a single scalar value, one has to condense these objectives in a process known as scalarization. Scalarization can for instance take the form of a weighted product $g = \prod g_i^{\alpha_i}$ or sum $g = \sum \alpha_i g_i$ of the individual objectives g_i , with the hyperparameters α_i describing its weight. Another common scalarization technique is c -constraint scalarization, where one seeks to reformulate the problem of optimizing multiple objectives into a problem of single-objective optimization conditioned on constraints. In this method the goal is to optimize one of the g_i , given some bounds on the other objectives. All of these techniques introduce some explicit bias in the optimization which may not necessarily repre-

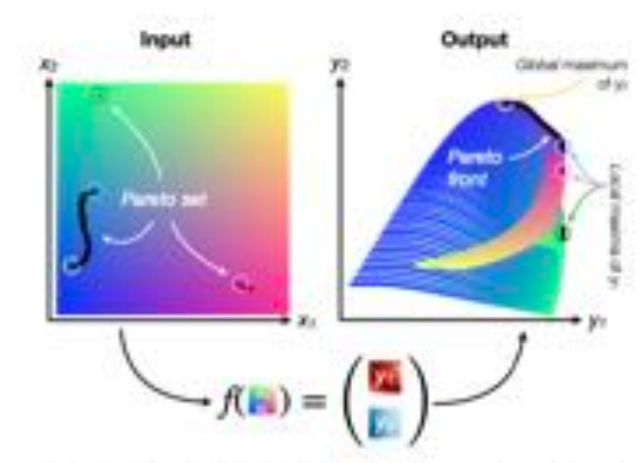


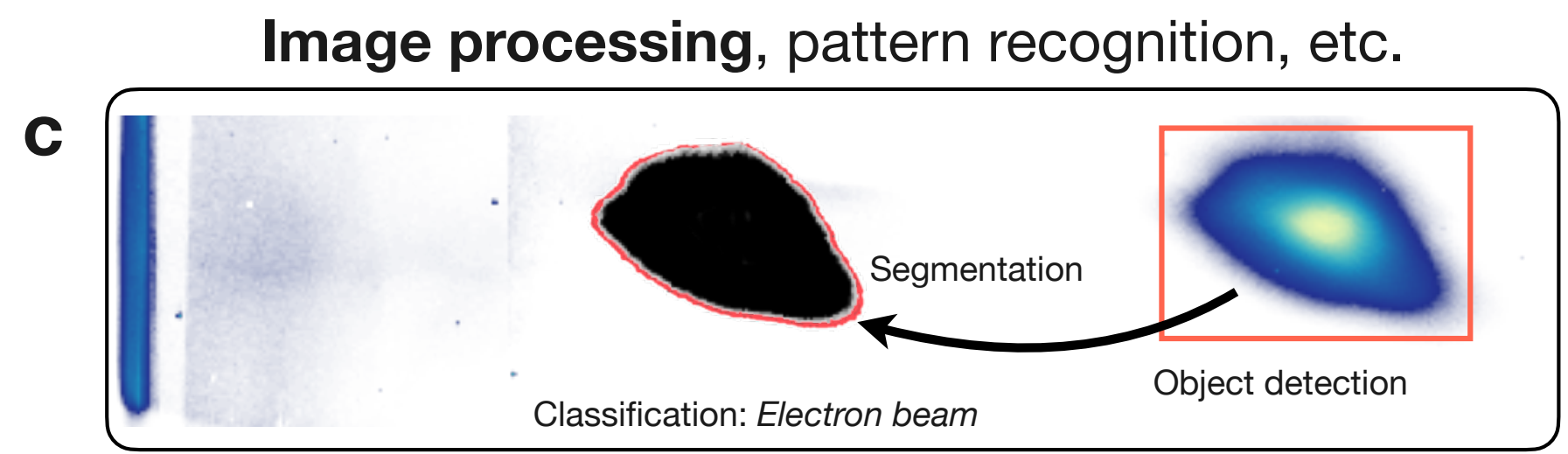
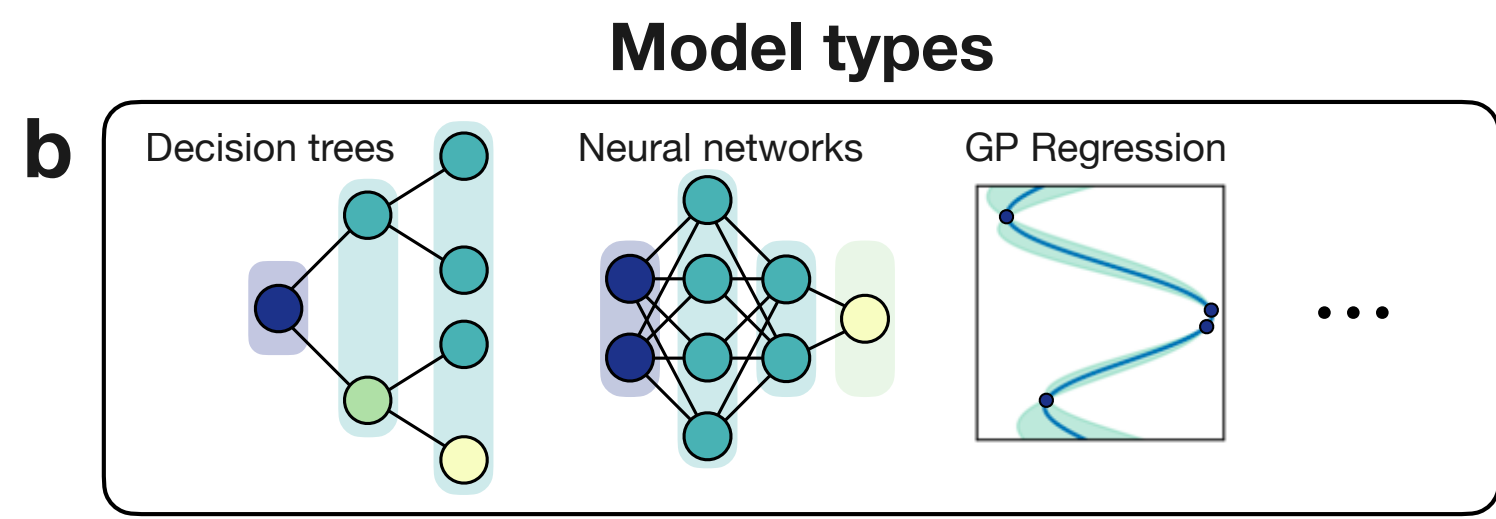
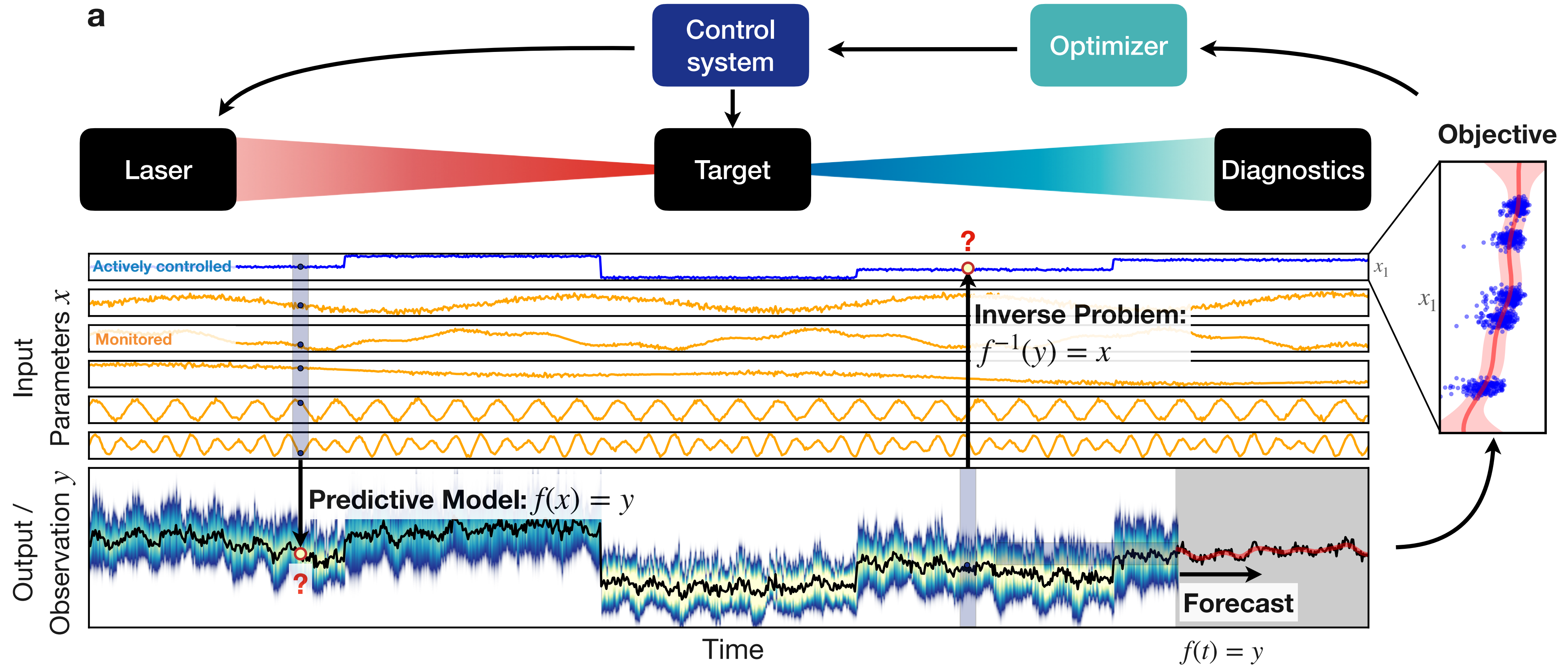
FIG. 12. Pareto front. Illustration how a multi-objective function $f(x) = y$ acts on a two-dimensional input space $x = (x_1, x_2)$ and transforms it to the objective space $y = (y_1, y_2)$ on the right. The entirety of possible input positions is uniquely color-coded on the left and the resulting position in the objective space is shown in the same color on the right. The Pareto-optimal solutions form the Pareto front, indicated on the right, whereas the corresponding set of coordinates in the input space is called the Pareto set. Note that both Pareto front and Pareto set may be continuously defined locally, but can also contain discontinuities when local maxima get involved. Adapted from Ishaq et al.²⁰⁷

sent the desired outcome. Because of this, the hyperparameters of the scalarization may have to be optimized themselves by running optimizations several times. A more general approach is Pareto optimization, where the entire vector of individual objectives $g = (g_1, \dots, g_N)$ is optimized. To do so, instead of optimizing individual objectives, it is based on the concept of dominance. A

1. A. Döpp et al. Data-driven Science and Machine Learning Methods in Laser-Plasma Physics, *arXiv:2212.00026* (2022), *HPLSE* (2023)

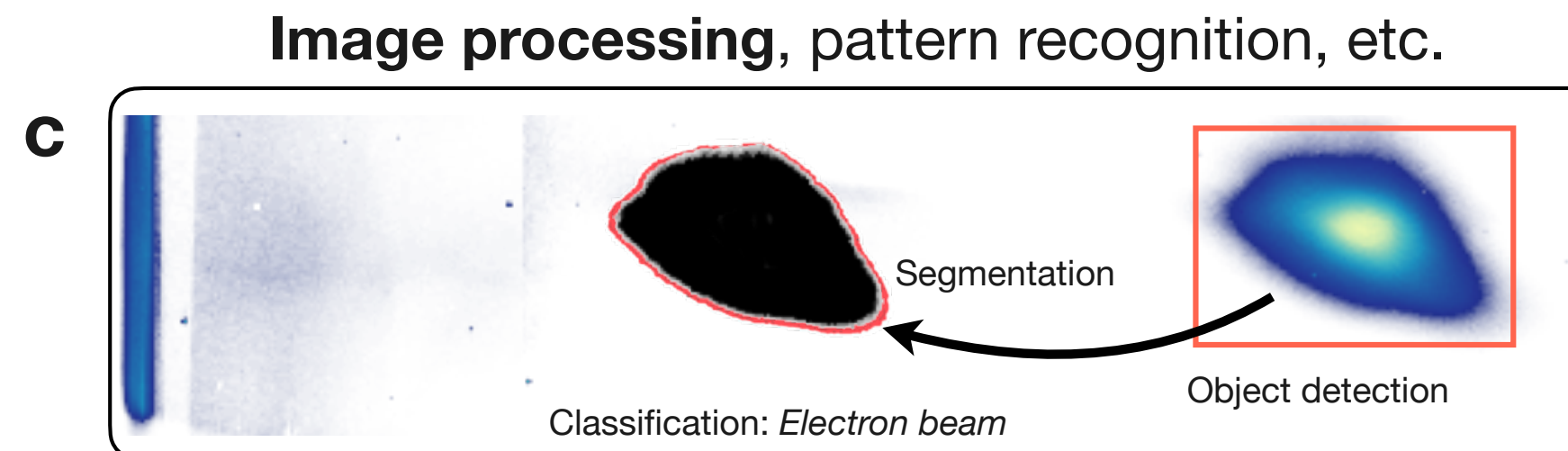
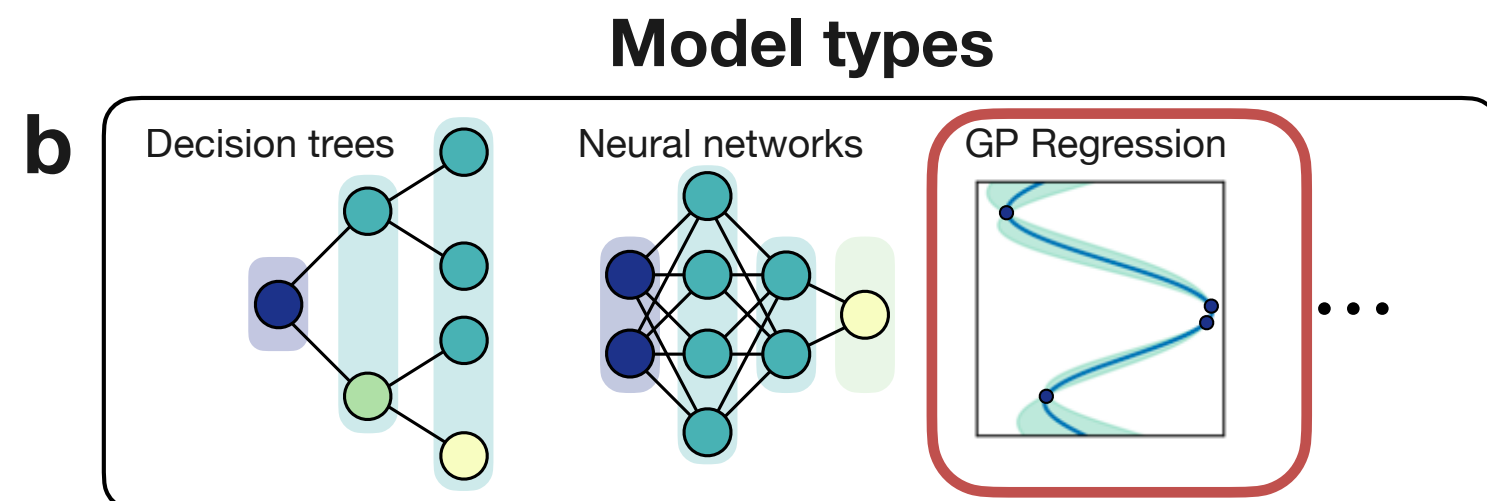
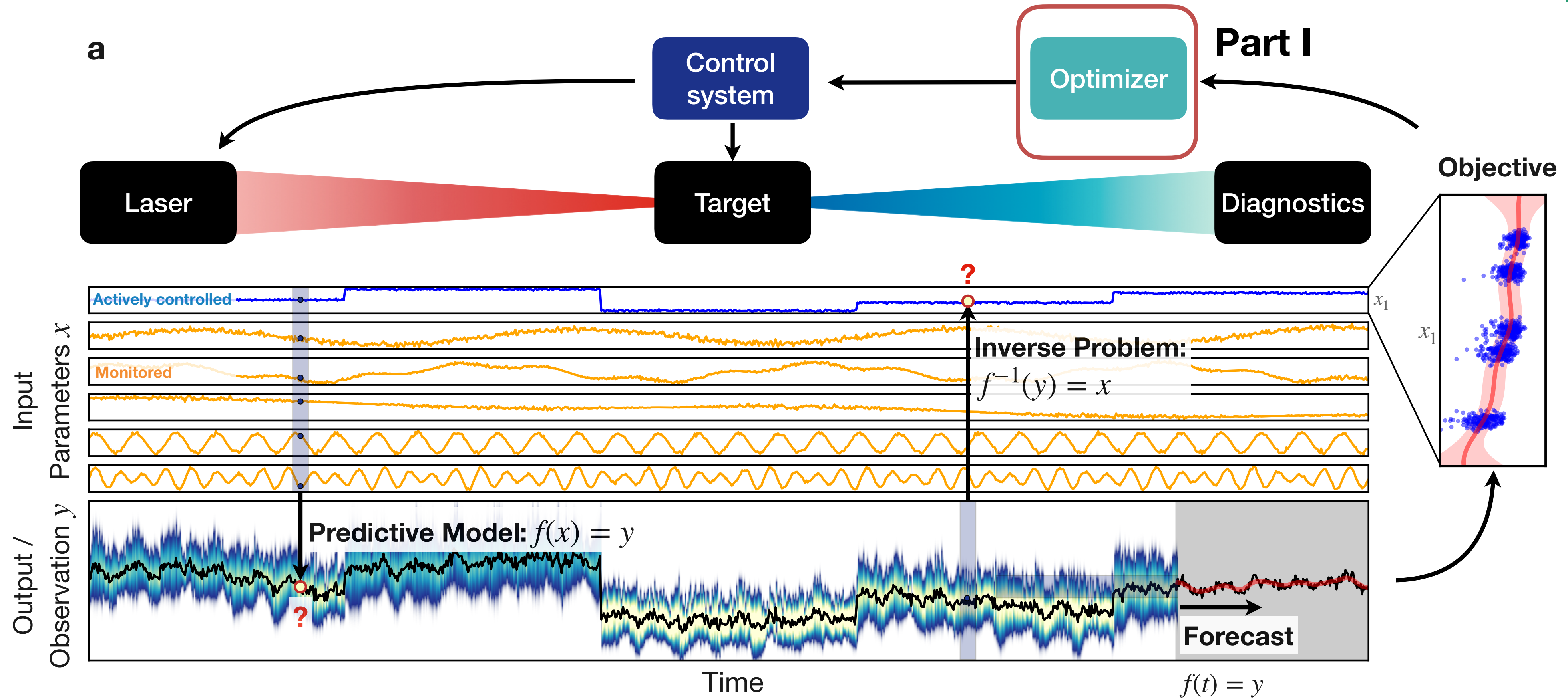
Machine learning strategies

General use cases



Machine learning strategies

General use cases



Part 1

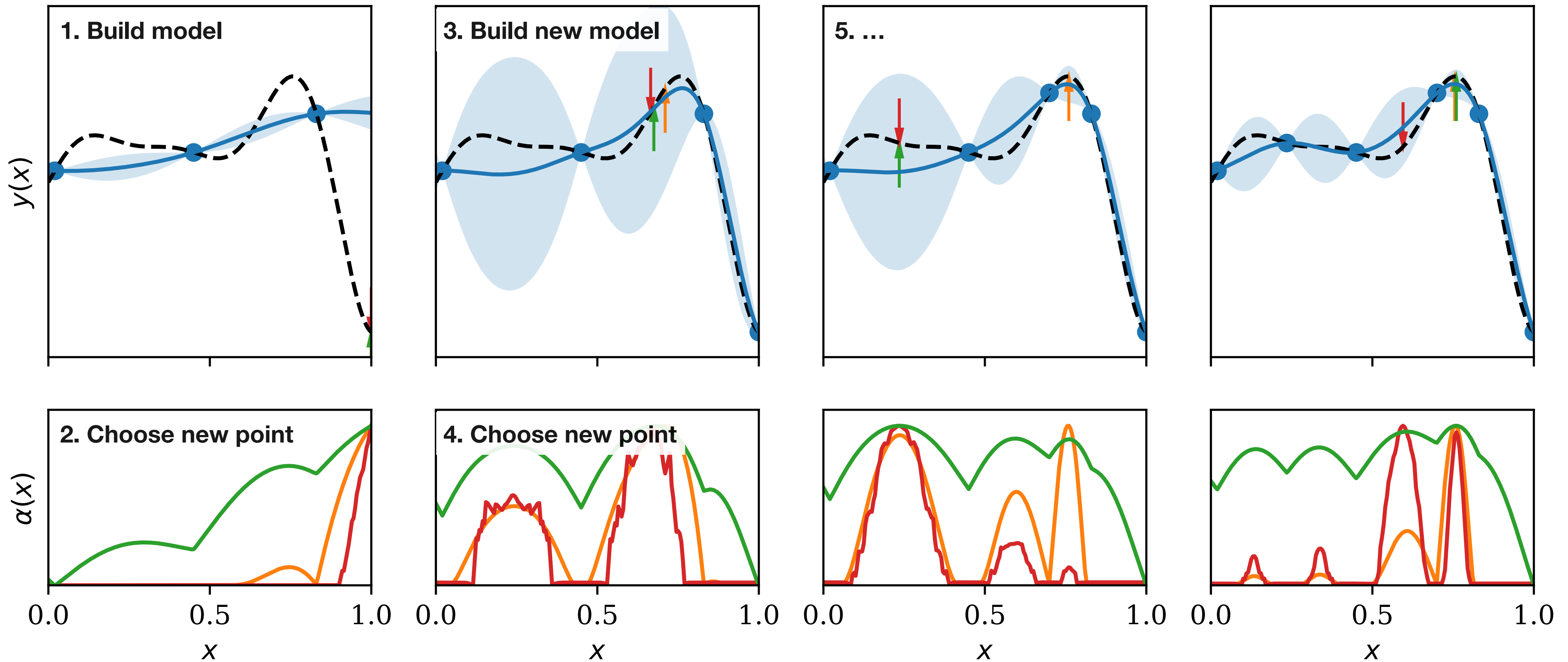
Multi-objective, multi-fidelity

Bayesian optimization

Bayesian optimization

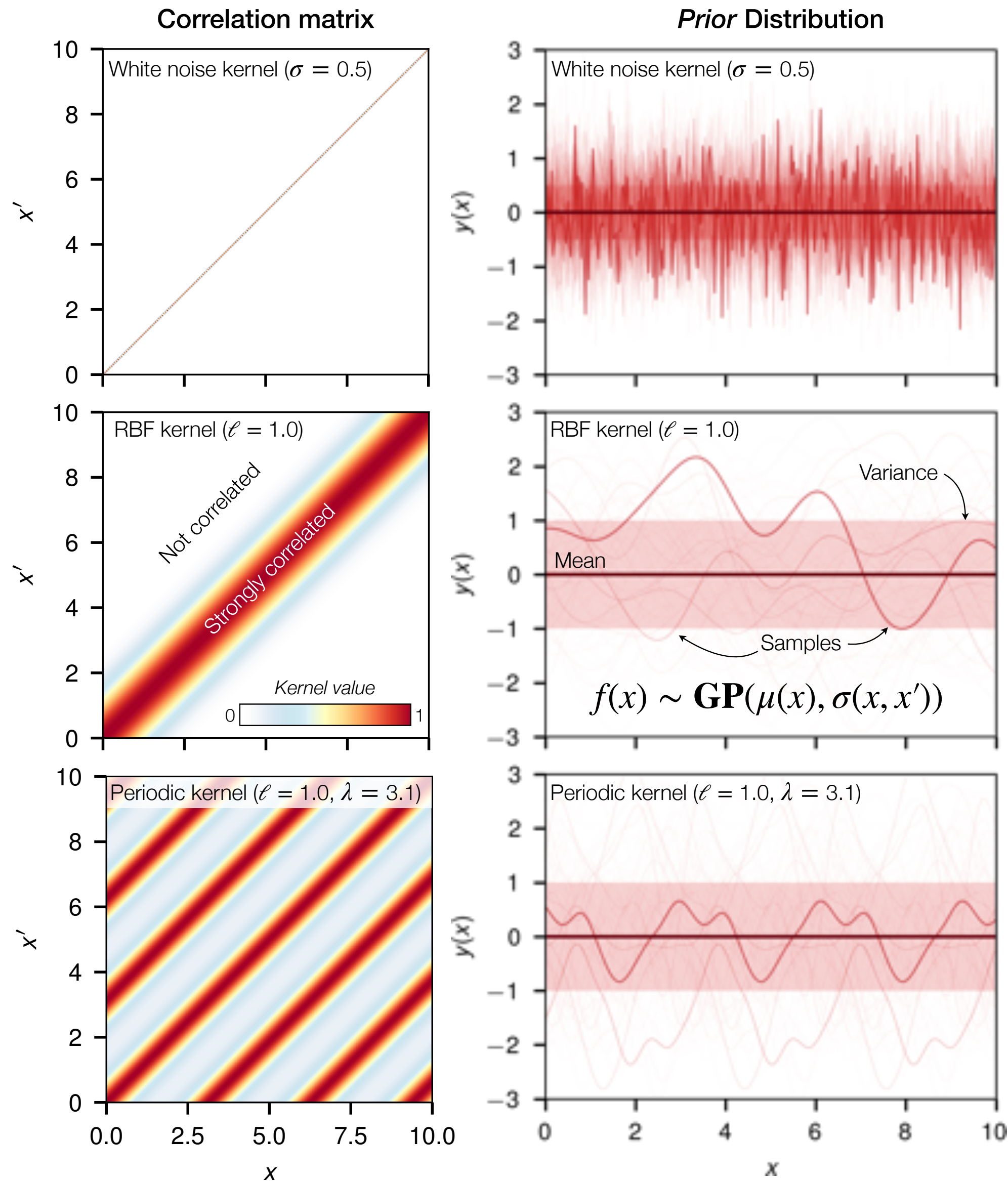
Sequential surrogate-based optimization

● Evaluated points - - - Ground truth — GP mean ■ GP std — EI — MES — UCB ($\kappa = 2$)



Gaussian process regression

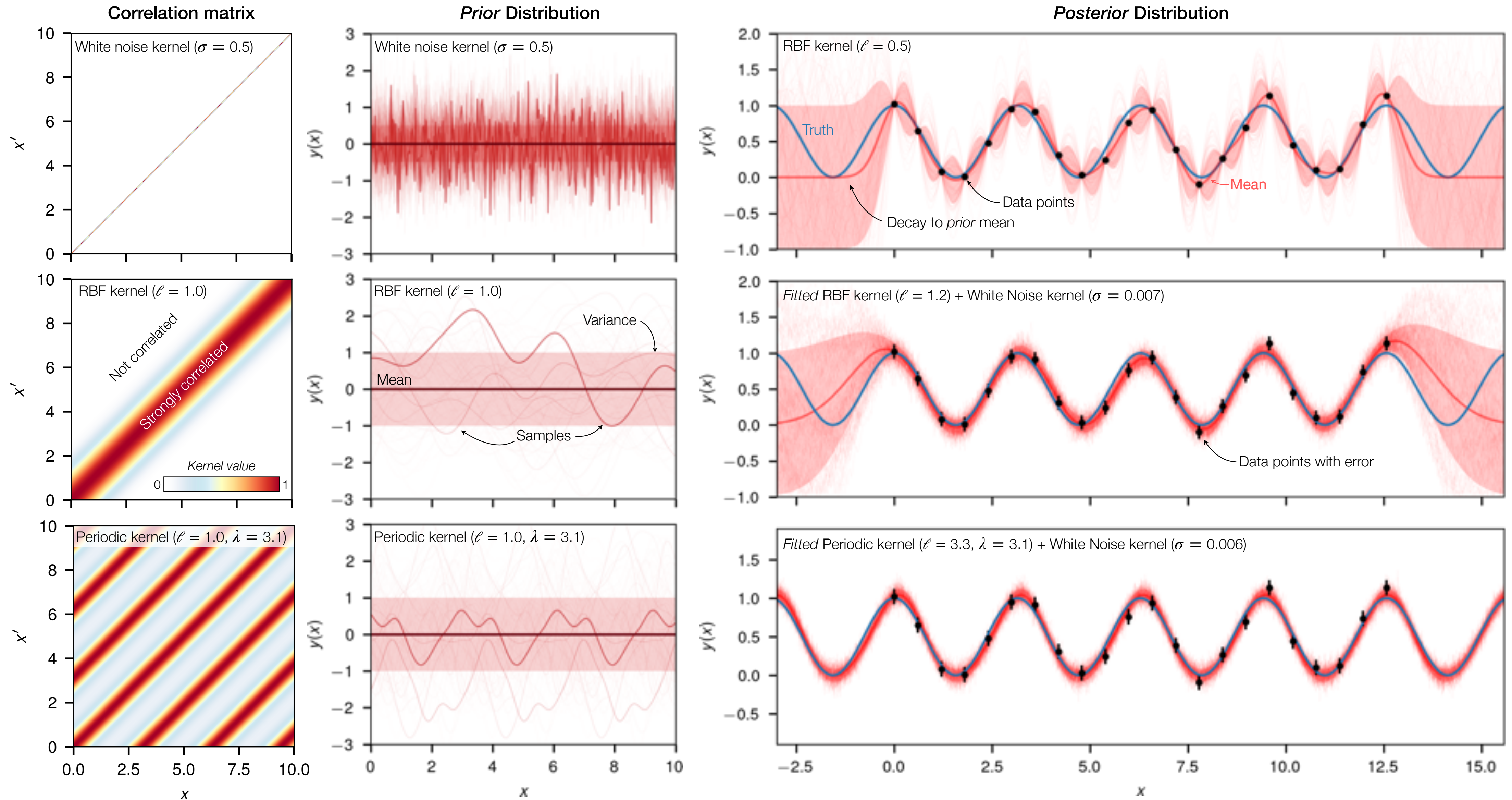
Modeling functions via correlations



- **Non-parametric method:** Predicts function values based on observed data without a predetermined model.
- **Covariance function/Kernel:** Defines the relationship between points, capturing their correlations.
- **Probabilistic description:** Provides a full description of the function, including mean and uncertainty.

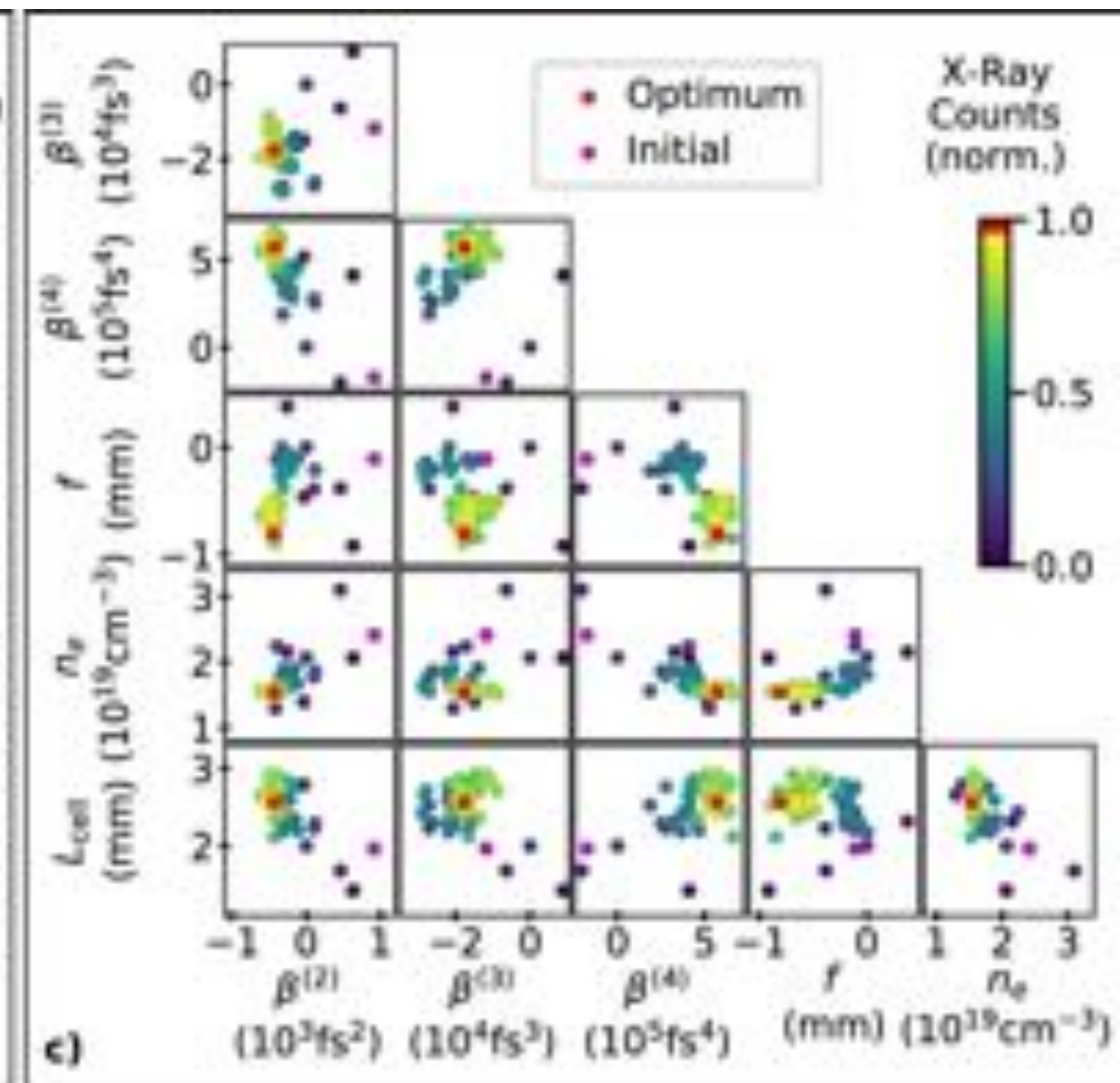
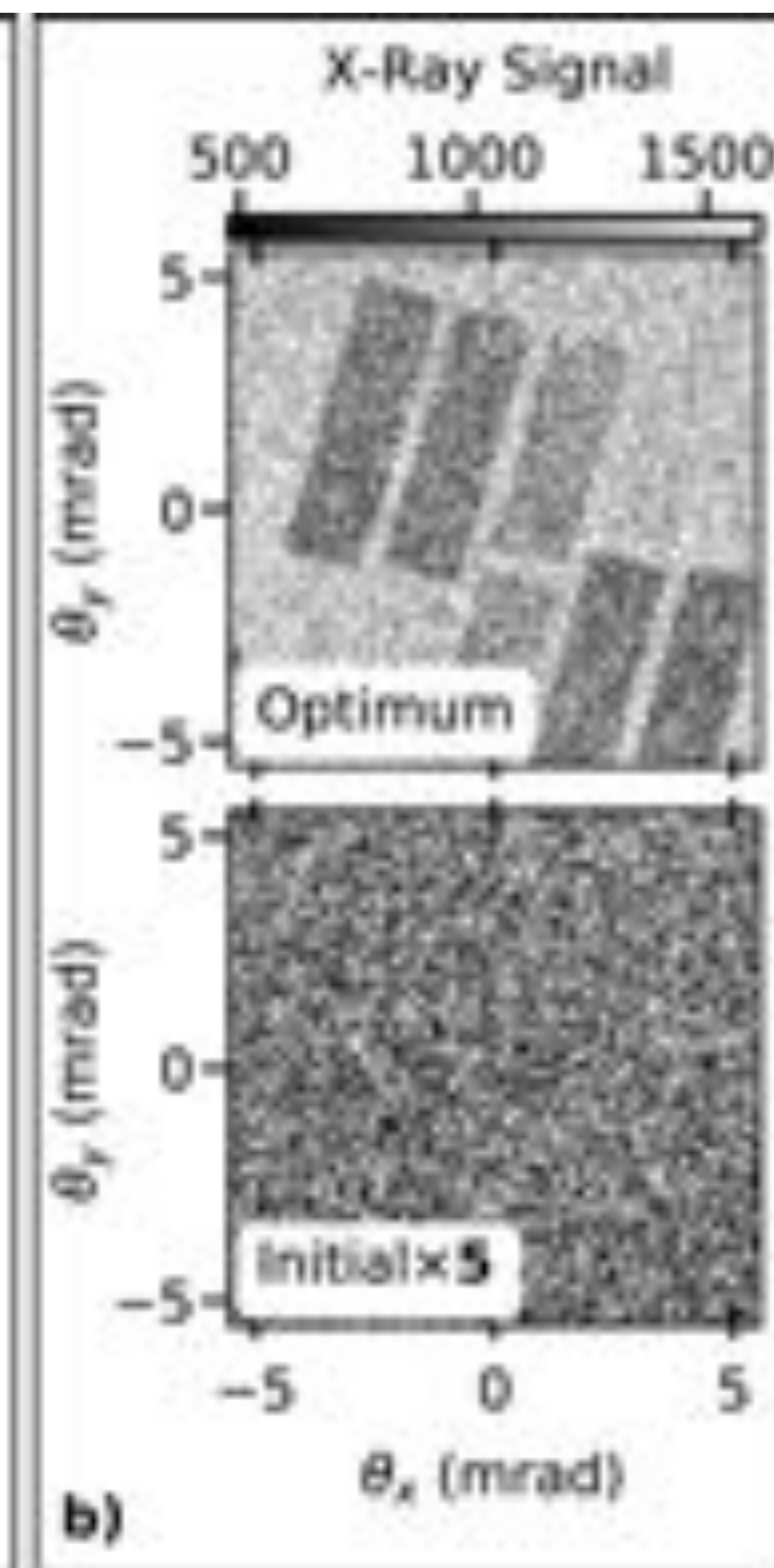
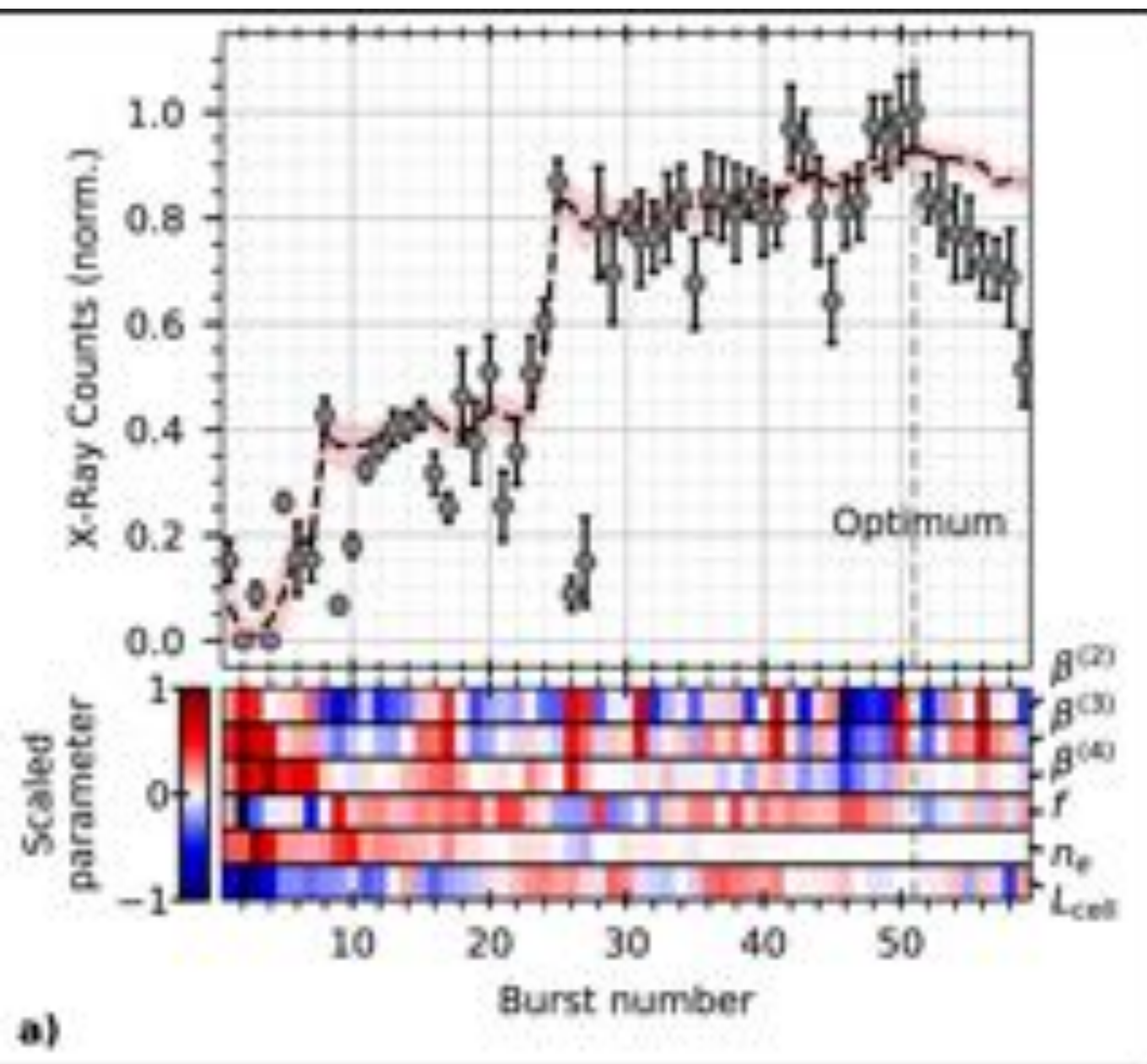
Gaussian process regression

Modeling functions via correlations



Bayesian optimization

First experimental results in laser-plasma acceleration



Multi-objective, multi-fidelity

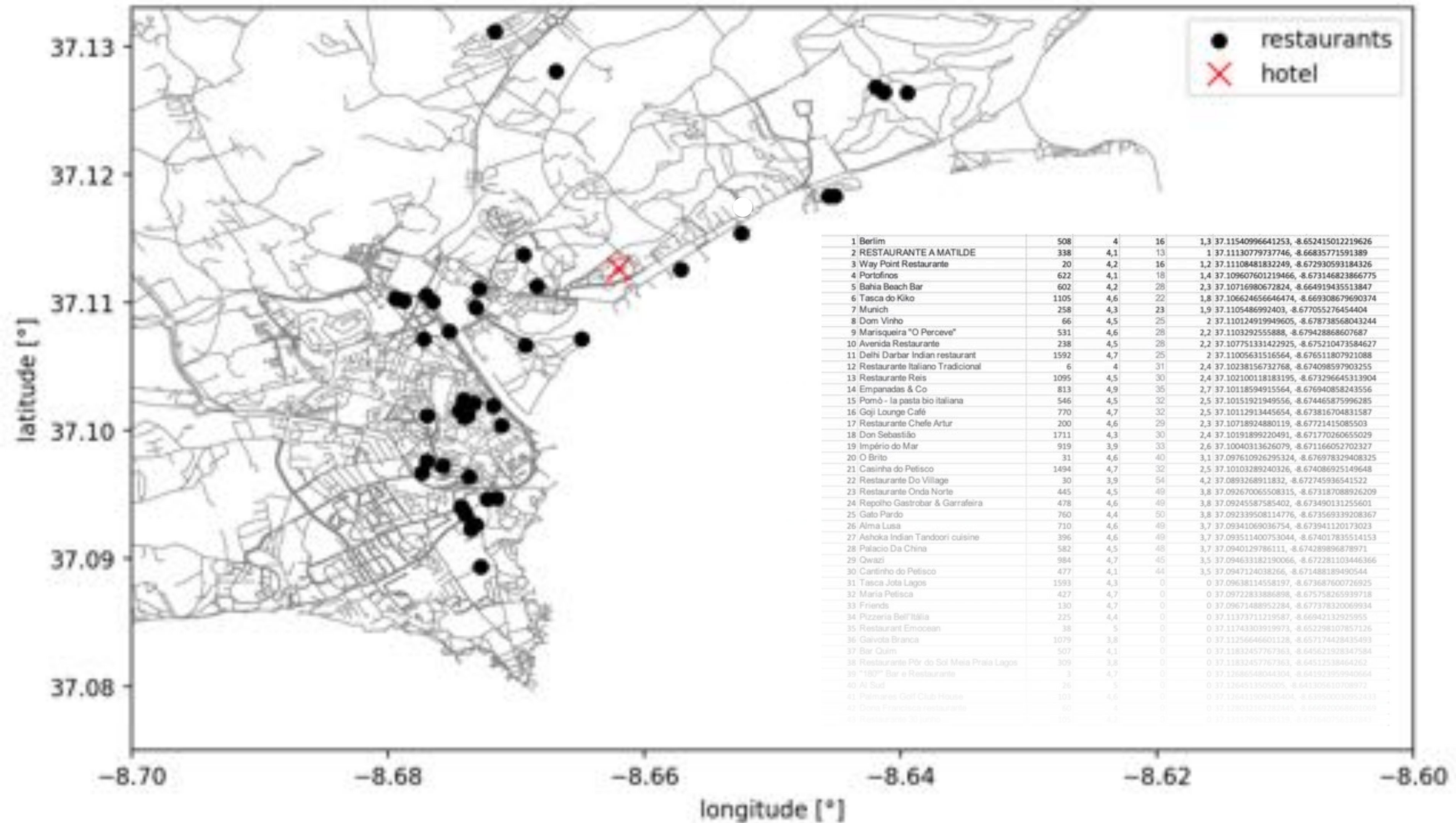
Bayesian optimization



The dinner problem

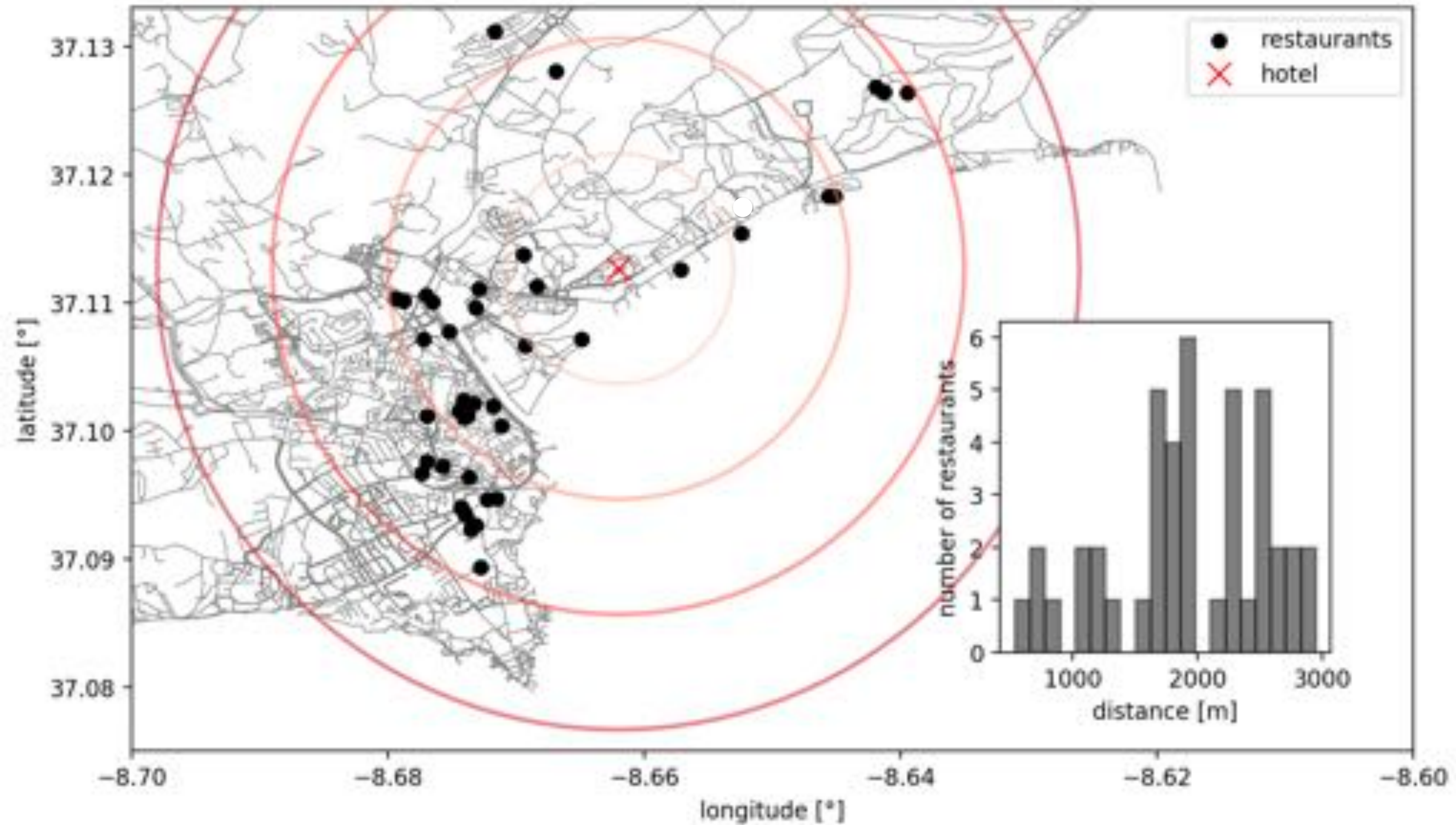
Multi-objective optimization

The dinner problem



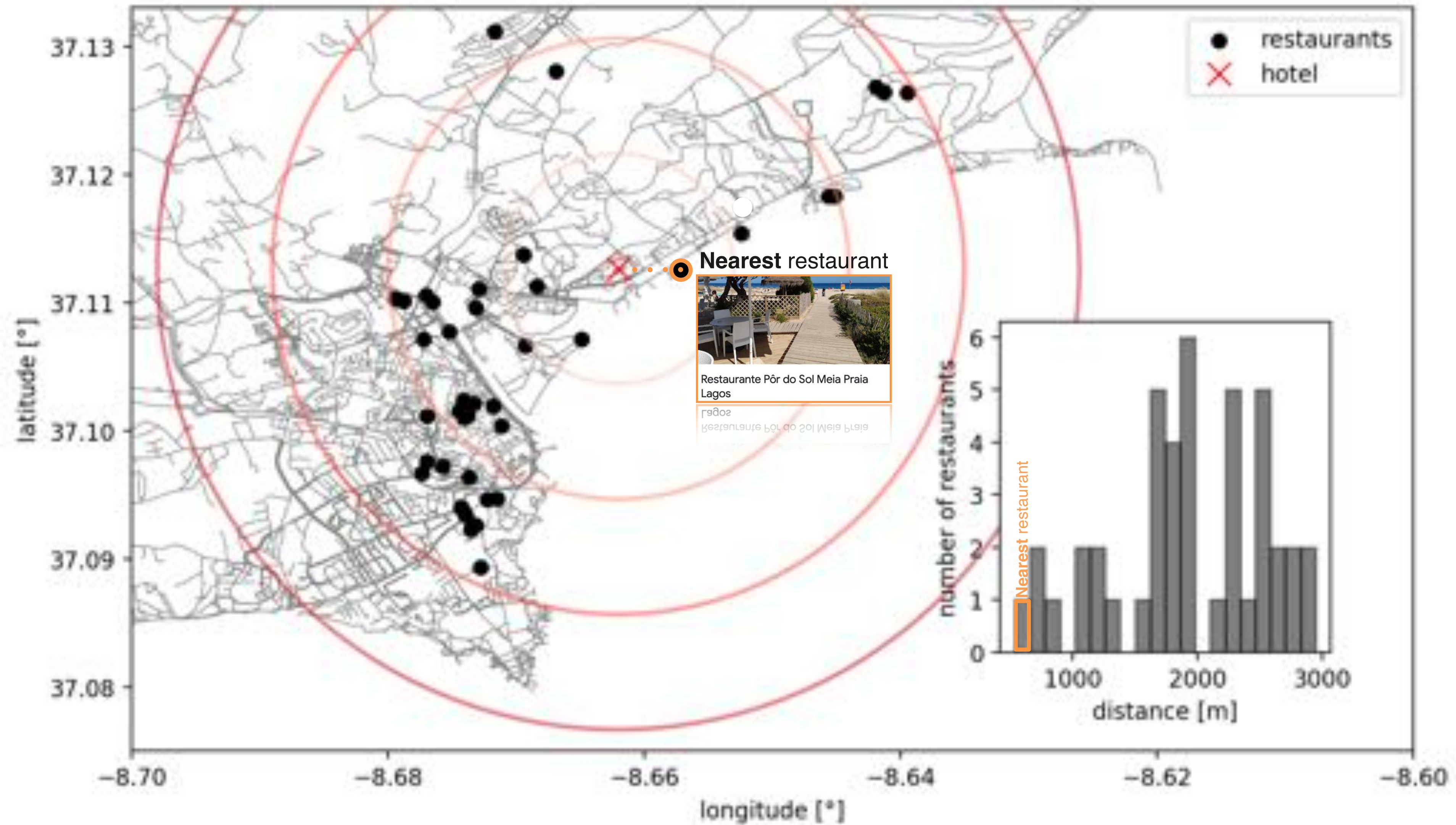
Multi-objective optimization

The dinner problem



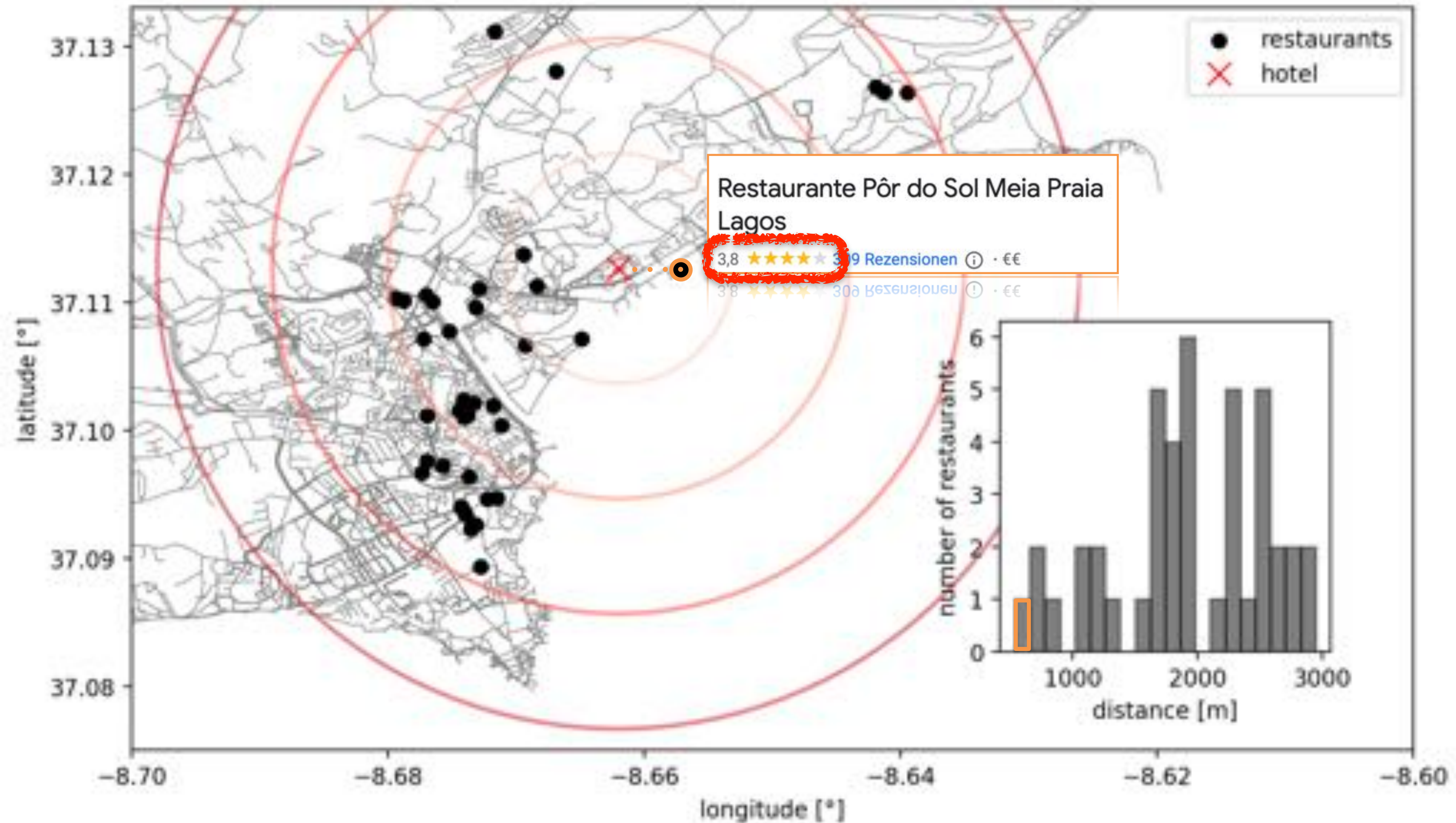
Multi-objective optimization

The dinner problem



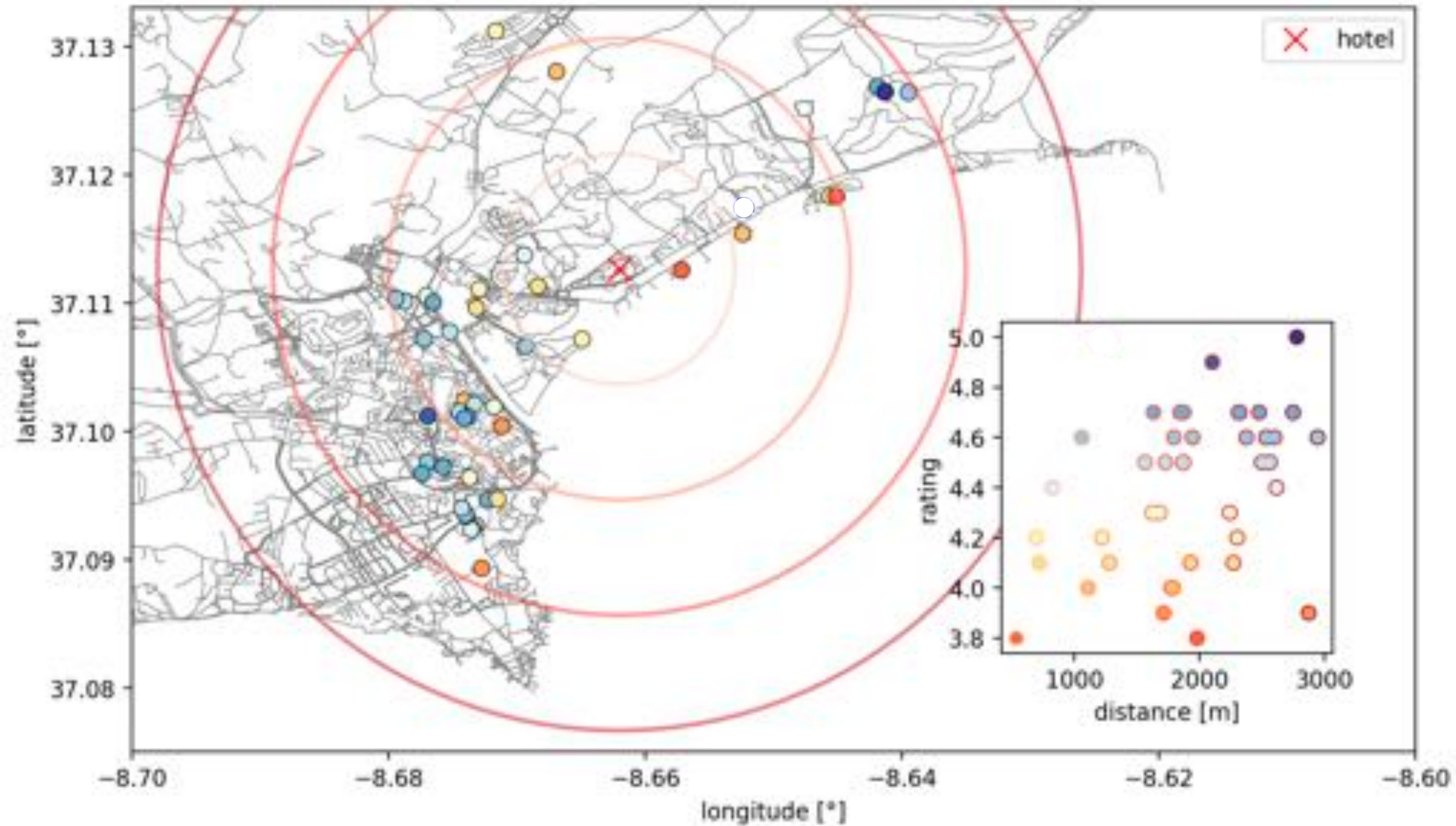
Multi-objective optimization

The dinner problem



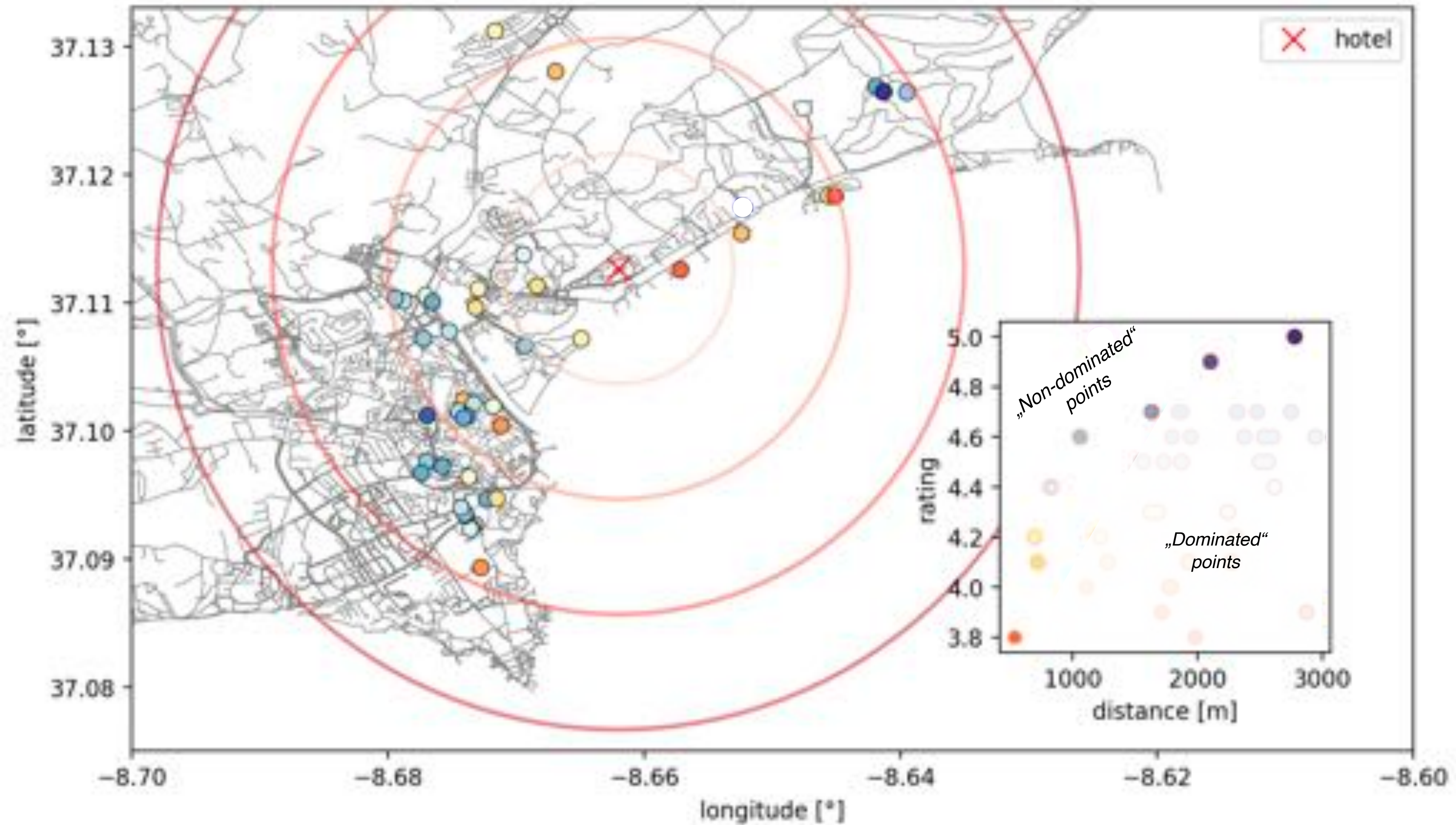
Multi-objective optimization

The dinner problem



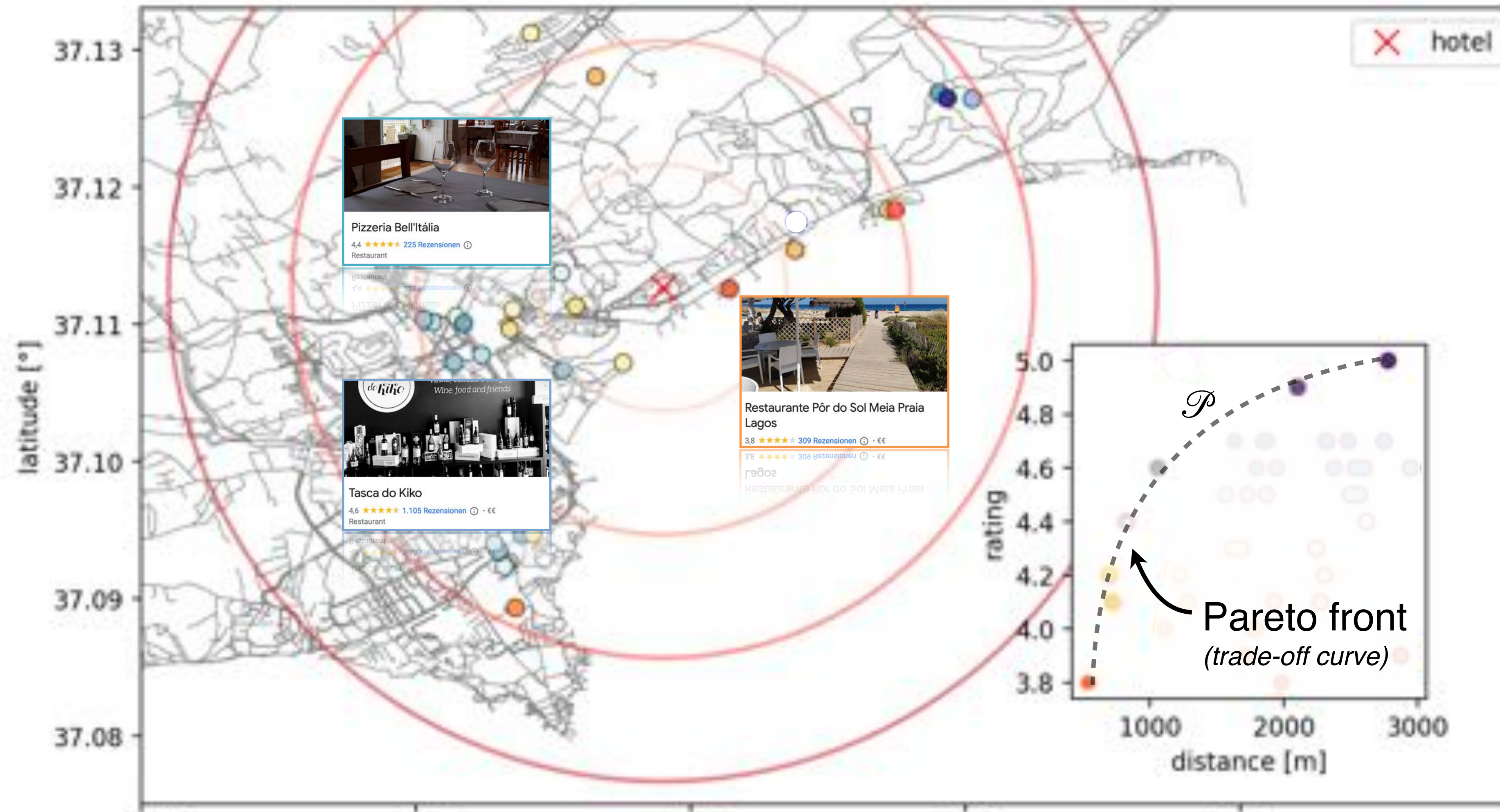
Multi-objective optimization

The dinner problem



Multi-objective optimization

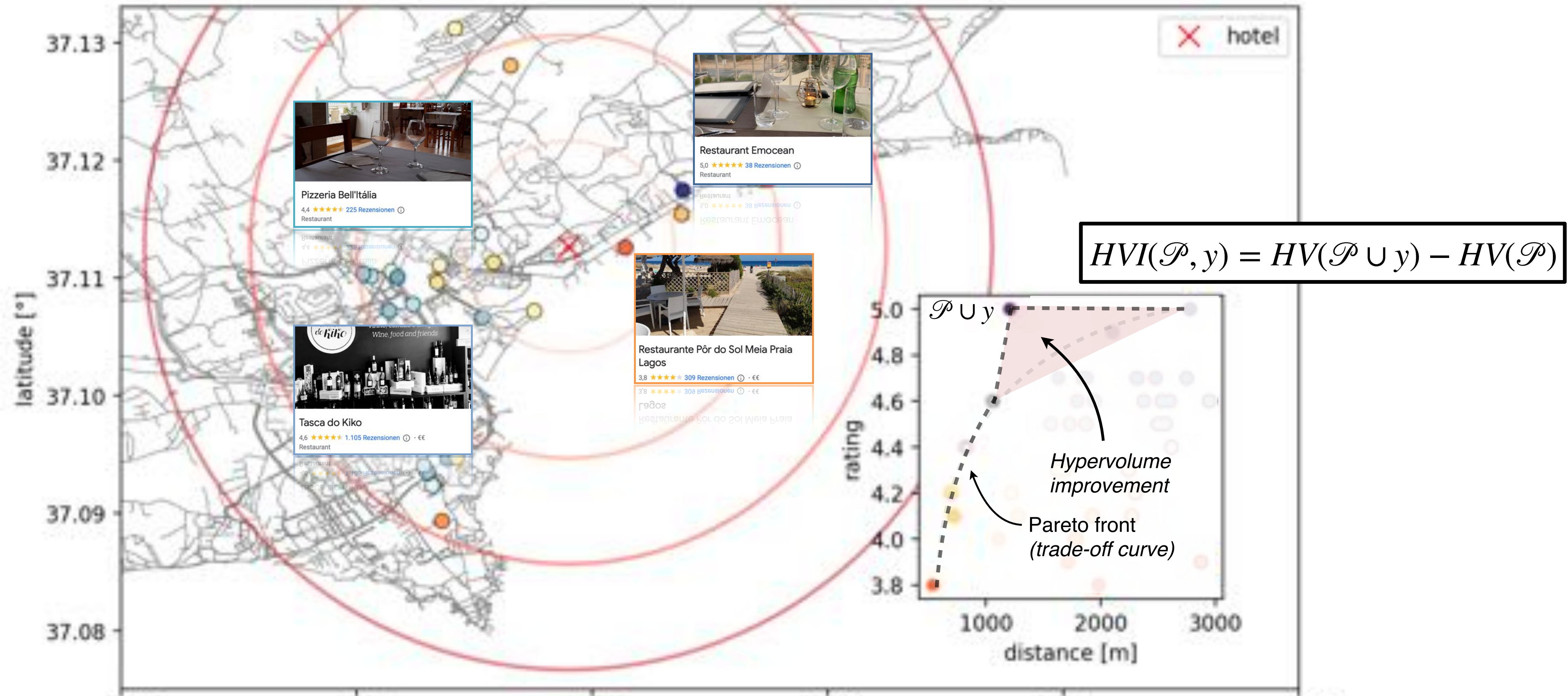
The dinner problem



In *multi-objective* optimization we have **multiple (competing) goals** with **different trade-offs**.

Multi-objective optimization

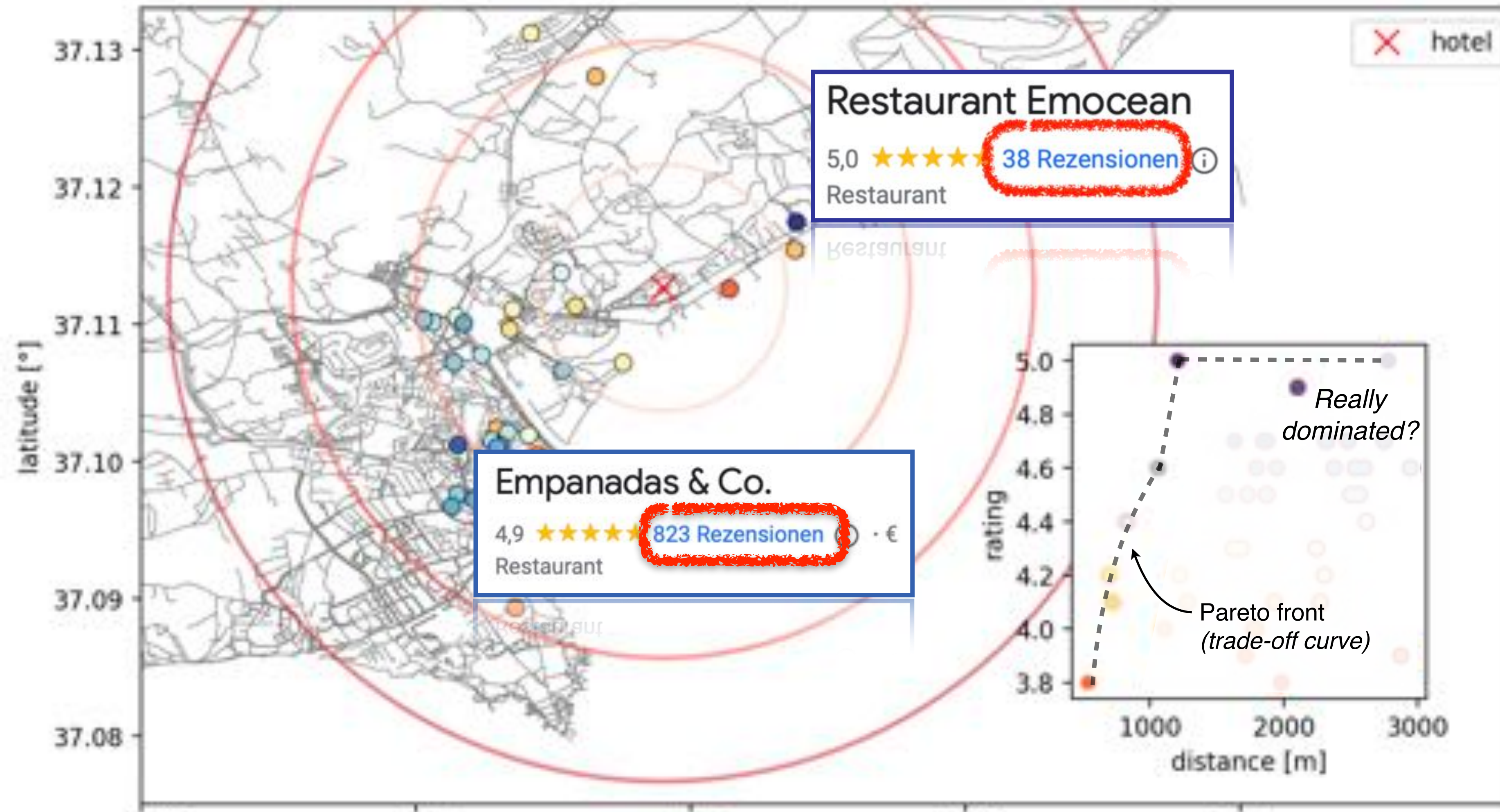
The dinner problem



In *multi-objective* optimization we have **multiple (competing) goals** with **different trade-offs**.

Multi-fidelity optimization

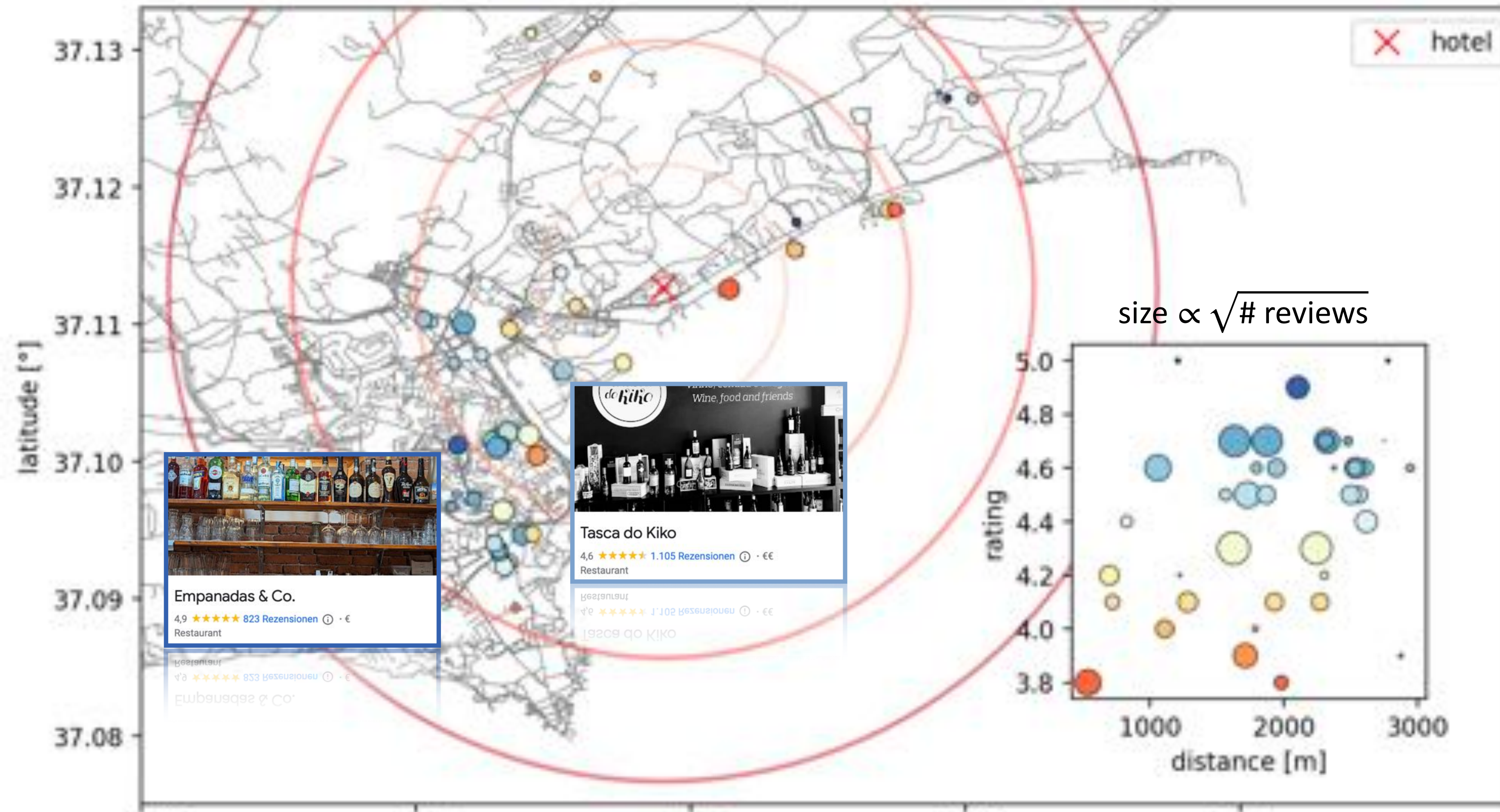
The dinner problem



In *multi-fidelity* optimization we have **different confidence in measurements**.

Multi-fidelity optimization

The dinner problem



In *multi-fidelity* optimization we have **different confidence in measurements**, thus **spanning another dimension** that represents how much we *trust* the point.

Multi-objective, multi-fidelity

Bayesian optimization

applied to laser-plasma acceleration

Multi-objective multi-fidelity optimization

Optimization of electron beam properties (*FBPIC simulations*)



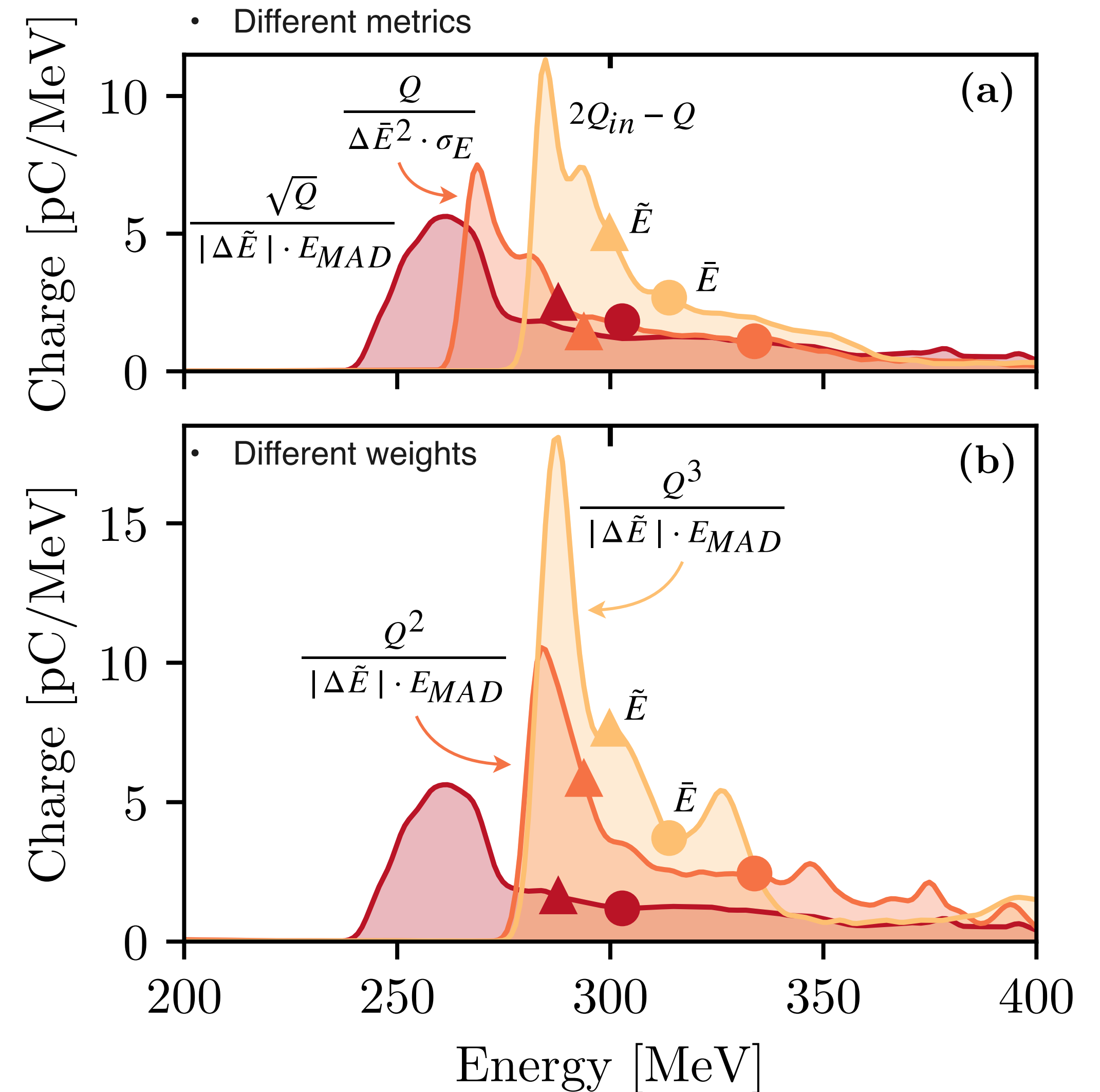
- We want to optimize three electron beam parameters:
 - Charge Q (total charge, charge within FWHM, etc.)
 - Bandwidth (standard deviation σ_E , median absolute deviation E_{MAD} , etc.)
 - Distance to a target energy $|E_{target} - E|$
(using mean energy, median energy, peak energy, etc.)

Multi-objective multi-fidelity optimization

Optimization of electron beam properties (*FBPIC simulations*)

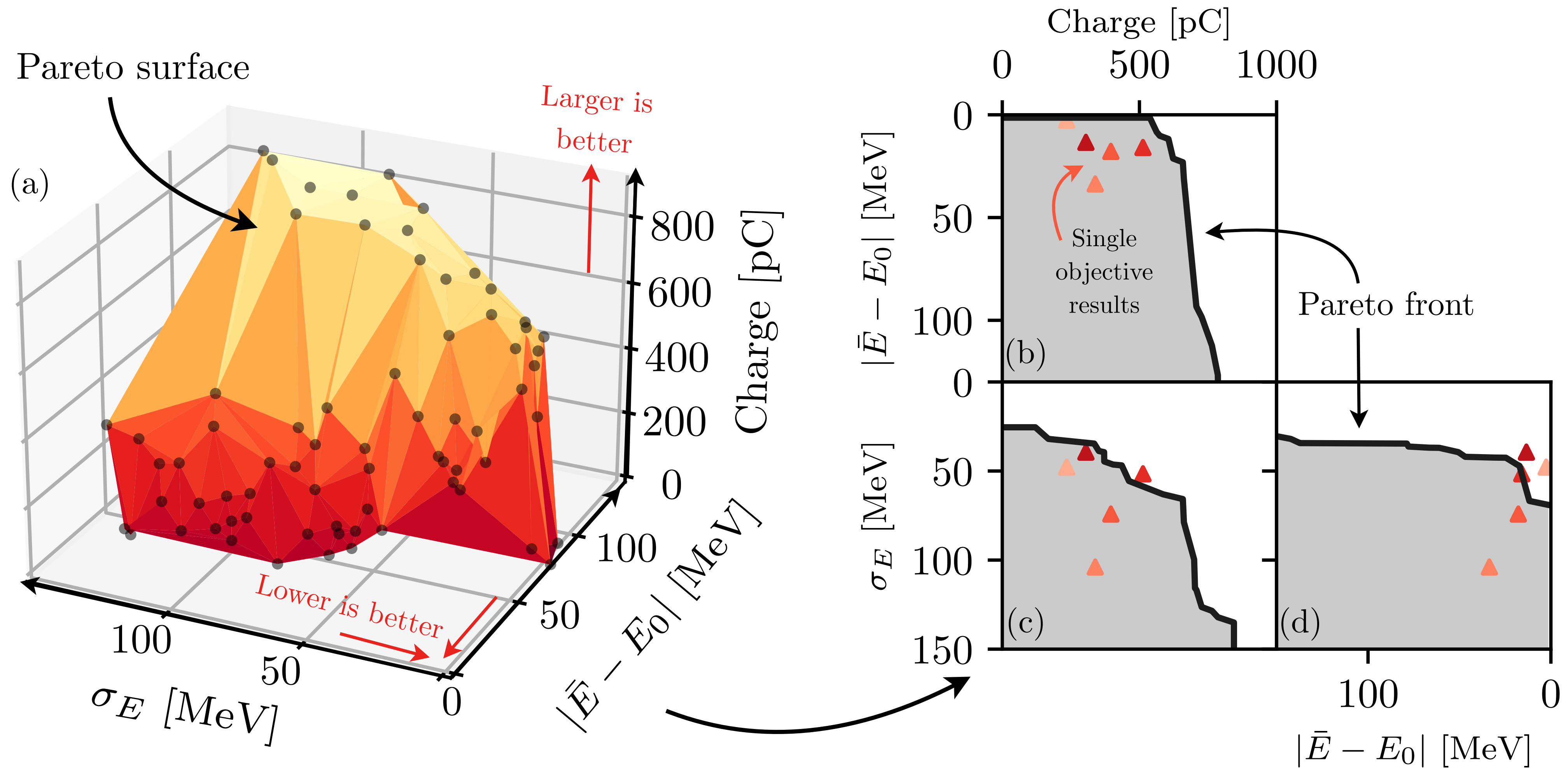


- We want to optimize three electron beam parameters:
 - Charge Q (total charge, charge within FWHM, etc.)
 - Bandwidth (standard deviation σ_E , median absolute deviation E_{MAD} , etc.)
 - Distance to a target energy $|E_{target} - E|$ (using mean energy, median energy, peak energy, etc.)
- We can use the simulation resolution as our fidelity, i.e. we trust a high-resolution simulation more than a low-resolution simulation (*including low-res gives one order of magnitude speed-up*)
- Choosing **different metrics or weights** for each objective **changes the outcome in an *a priori* unknown way!**



Multi-objective multi-fidelity optimization

Optimization of electron beam properties (*FBPIC simulations*)



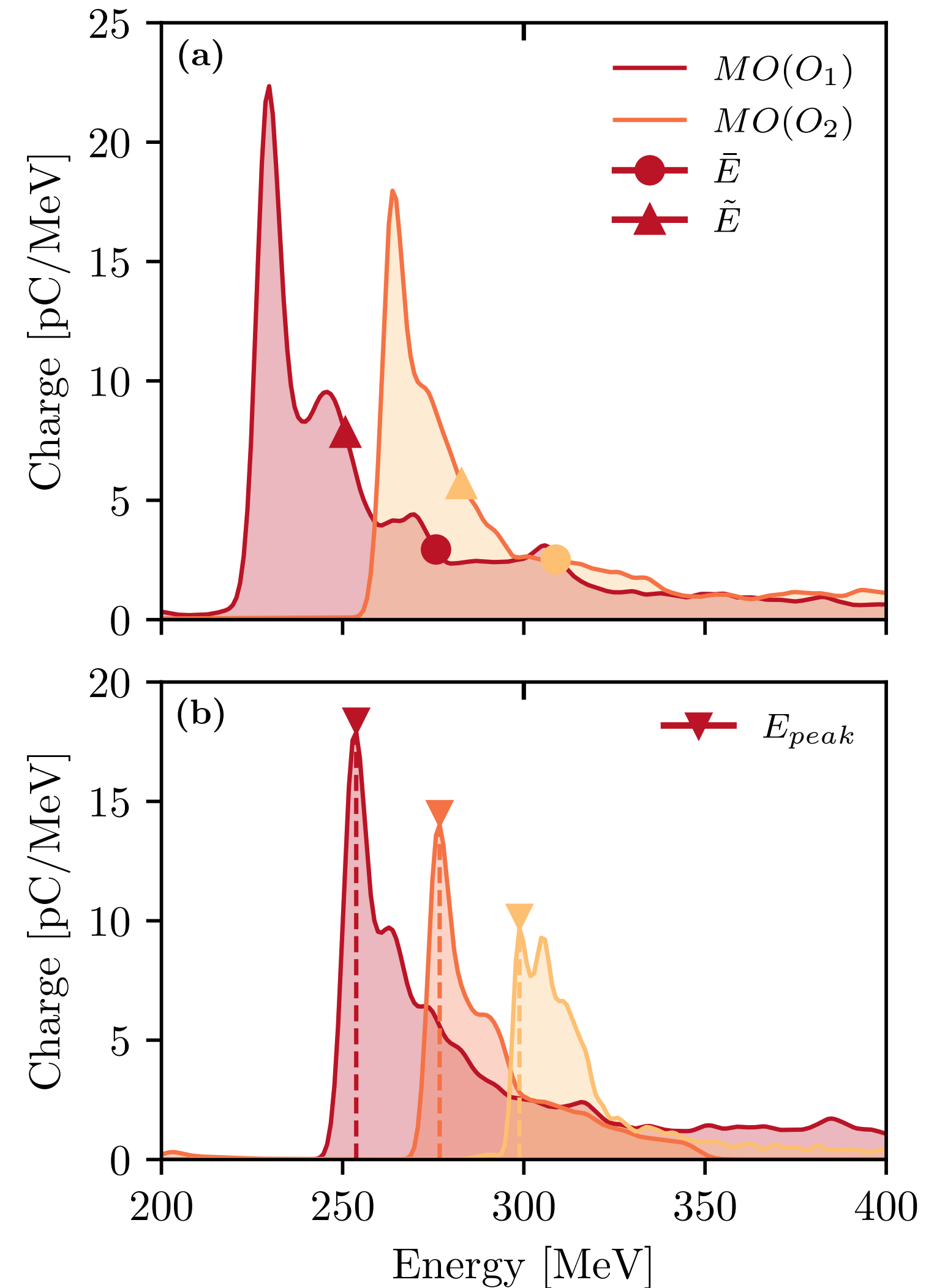
1. Irshad, F., Karsch, S., & Döpp, A. **EHVI for simultaneous multi-objective and multi-fidelity optimization.** *arXiv preprint arXiv:2112.13901* (2021)

2. Irshad, F., Karsch, S., & Döpp, A. **Multi-objective and multi-fidelity Bayesian optimization of laser-plasma acceleration.** *Phys. Rev. Research* 5, 013063 (2023)

Multi-objective multi-fidelity optimization

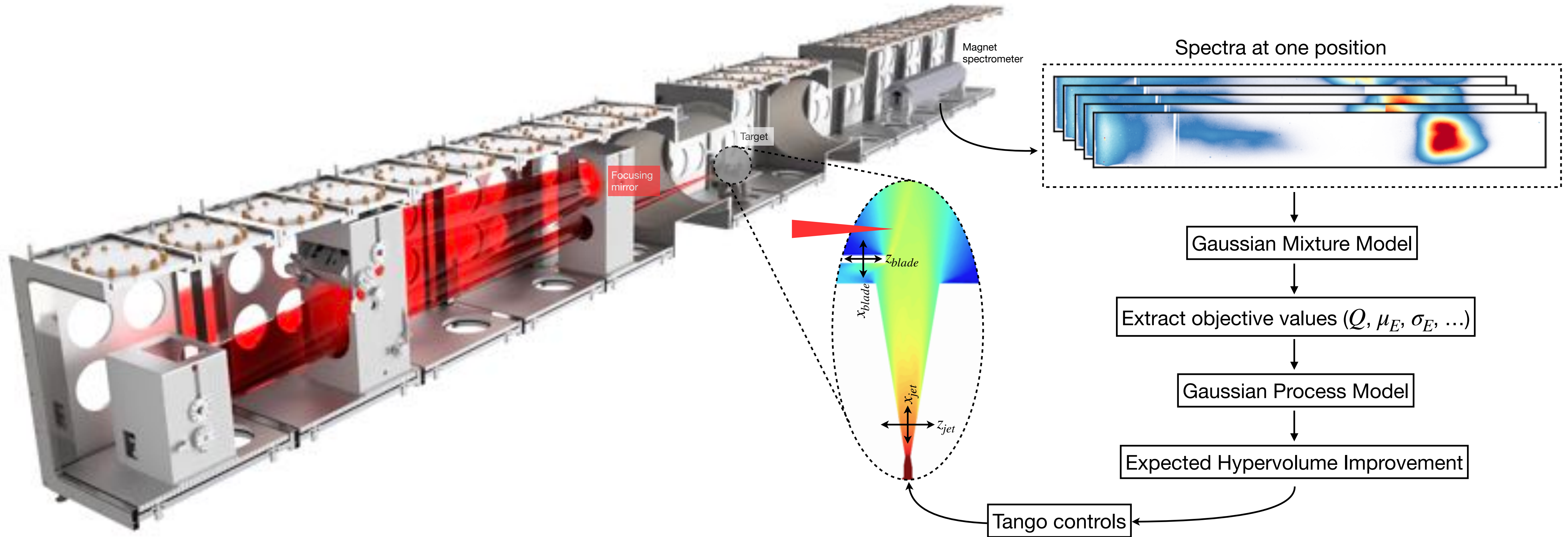
Optimization of electron beam properties (*FBPIC simulations*)

- Once the Pareto-optimal solutions are identified, we can choose from them what kind of beam we want.
- We can also use the model's data to **change parameters *a posteriori***, e.g. to **tune the beam energy**.



Multi-objective multi-fidelity optimization

Optimization of electron beam properties (*Experiment*)



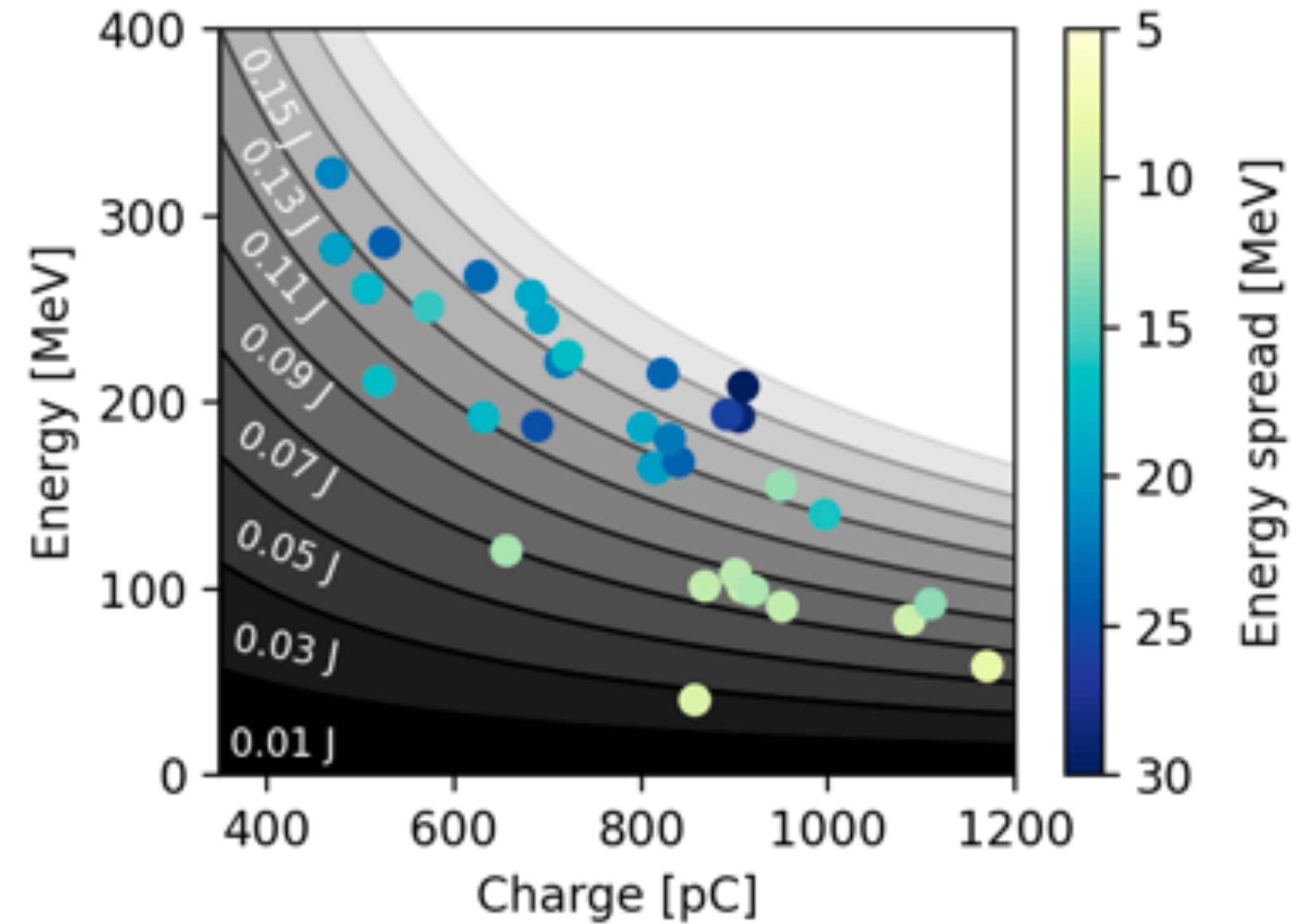
- N. Weiße et al. **Tango Controls and Data Pipeline for Petawatt Laser Experiments**, HPLSE, 10.1017/hpl.2023.17 (2023)
- F. Irshad, et al. **Pareto Optimization of a Laser Wakefield Accelerator** (*under review*)

Multi-objective multi-fidelity optimization

Optimization of electron beam properties (*Experiment*)



- Once the Pareto-optimal solutions are identified, we can choose from them what kind of beam we want.
- We observe that many of the Pareto-optimal solutions yield the **same laser-to-beam efficiency**.



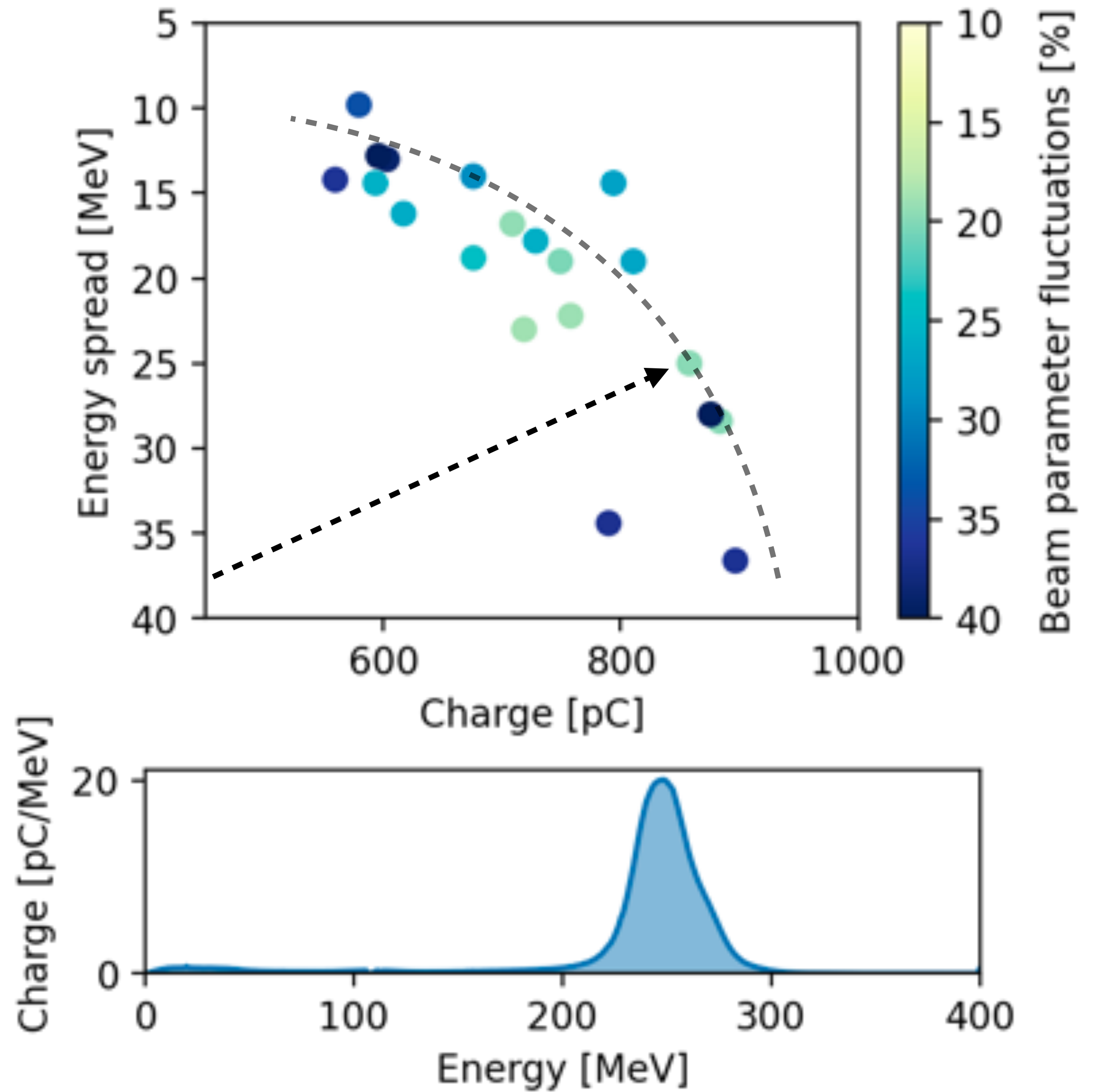
- N. Weiße et al. **Tango Controls and Data Pipeline for Petawatt Laser Experiments**, HPLSE, 10.1017/hpl.2023.17 (2023)
- F. Irshad, et al. **Pareto Optimization of a Laser Wakefield Accelerator** (*under review*)

Multi-objective multi-fidelity optimization

Optimization of electron beam properties (*Experiment*)



- Once the Pareto-optimal solutions are identified, we can choose from them what kind of beam we want.
- We can **select and exploit one particular solution** within the Pareto-optimal solutions by fitting $O_{select} = a_1 Q + a_2 \sigma_E + a_3 |E_{target} - E|$ such that it is maximized for the selected point.



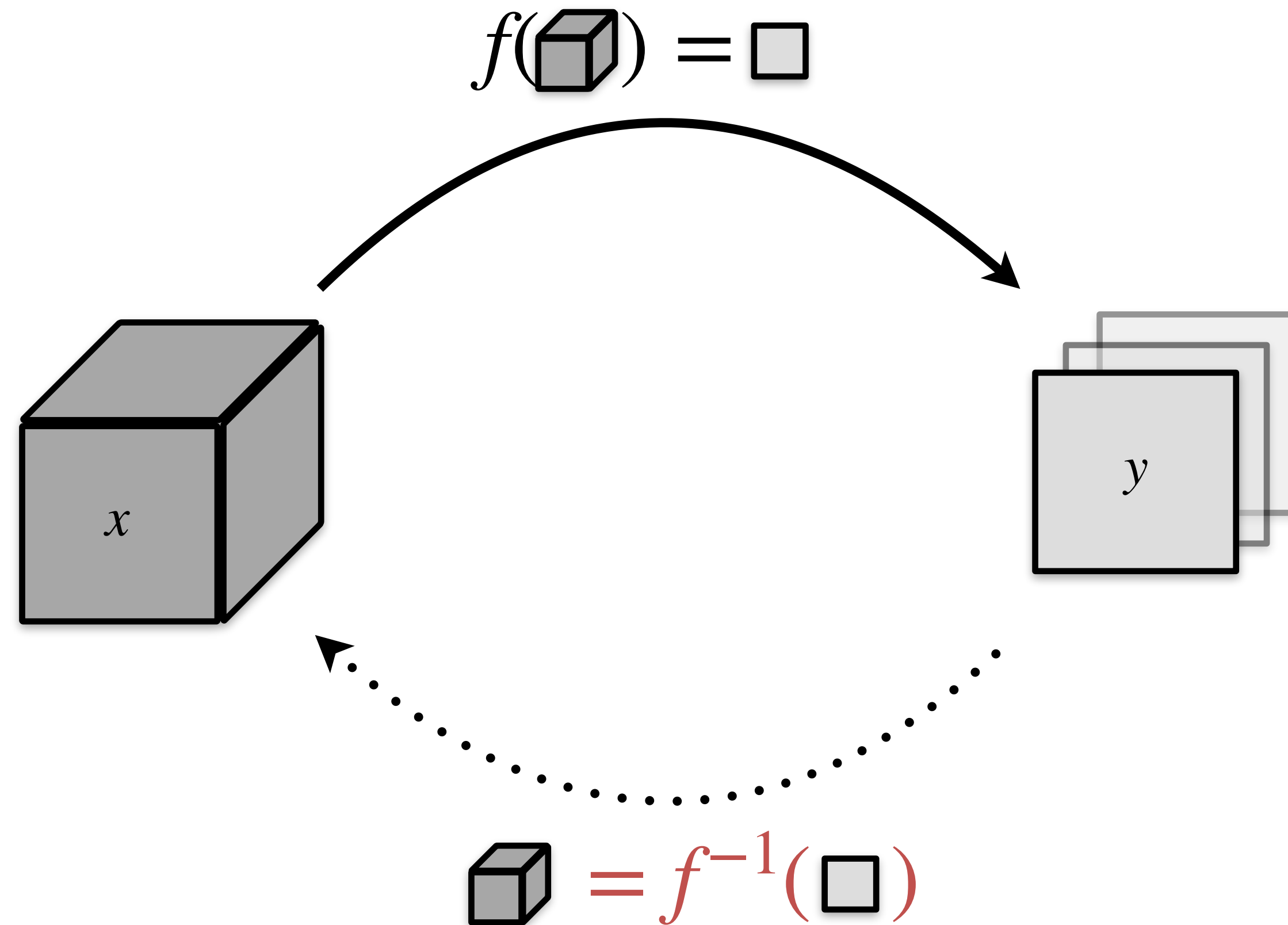
- N. Weiße et al. **Tango Controls and Data Pipeline for Petawatt Laser Experiments**, HPLSE, 10.1017/hpl.2023.17 (2023)
- F. Irshad, et al. **Pareto Optimization of a Laser Wakefield Accelerator** (*under review*)

Part 2

Inverse problems

Inverse Problems

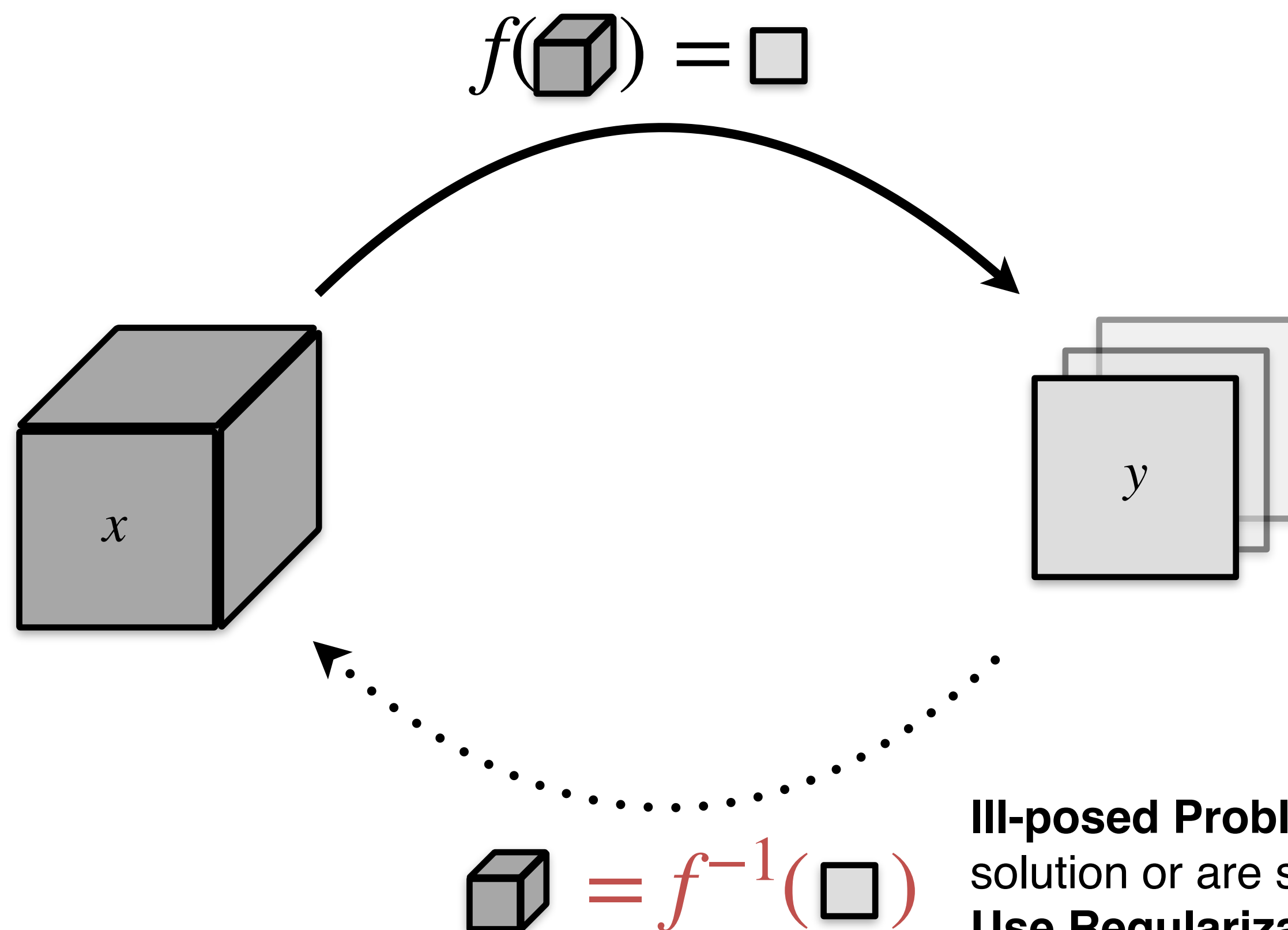
Determining cause from effect



Cause and Effect: Inverse problems involve determining the cause (e.g. 3D structure) from the observed effect (e.g. 2D projections).

Inverse Problems

Determining cause from effect



Ill-posed Problems: Inverse problems often lack a unique solution or are sensitive to input data.
Use Regularization to stabilize the solution by introducing additional information or assumptions.

Cause and Effect: Inverse problems involve determining the cause (e.g. 3D structure) from the observed effect (e.g. 2D projections).

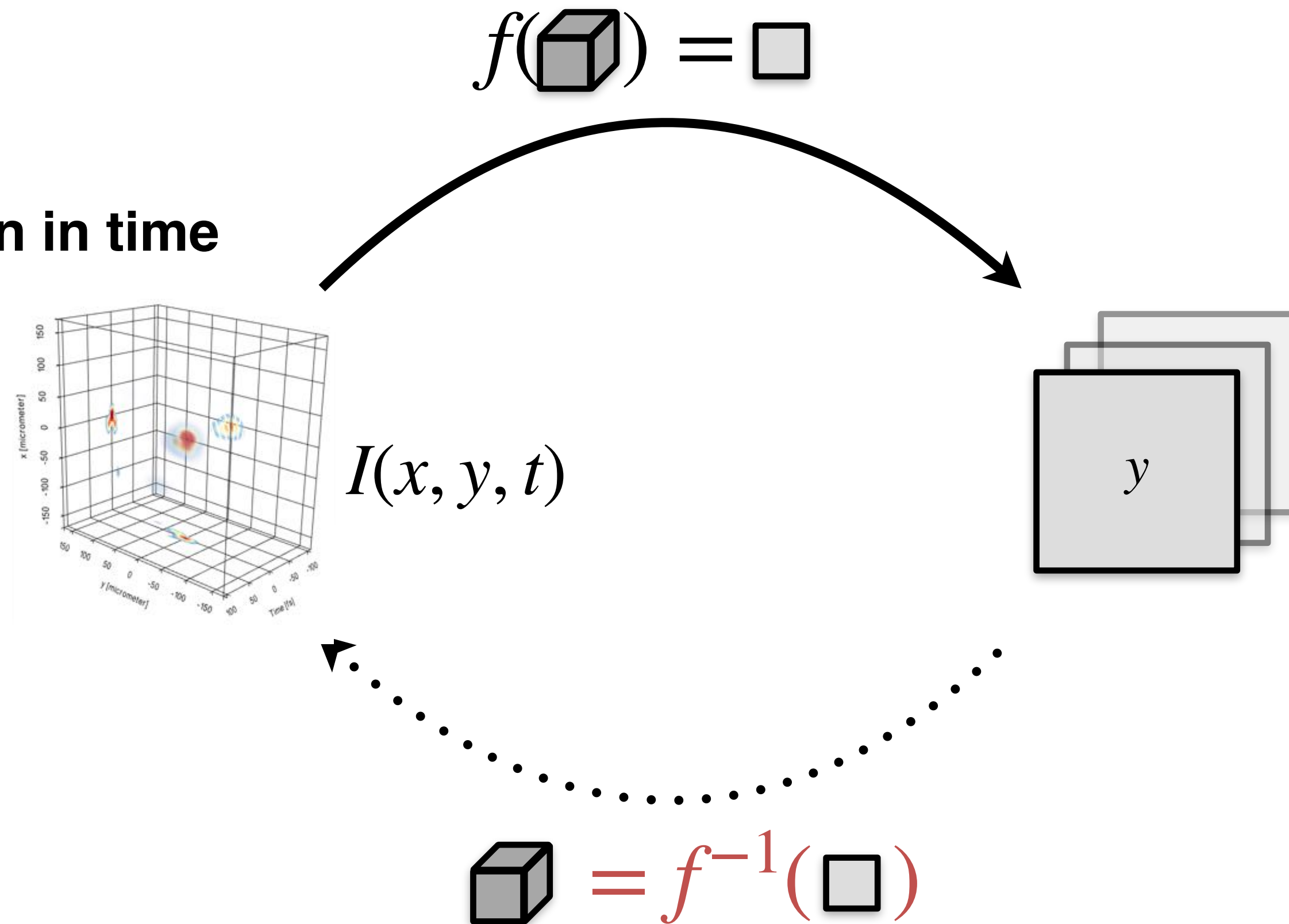
Inverse Problems

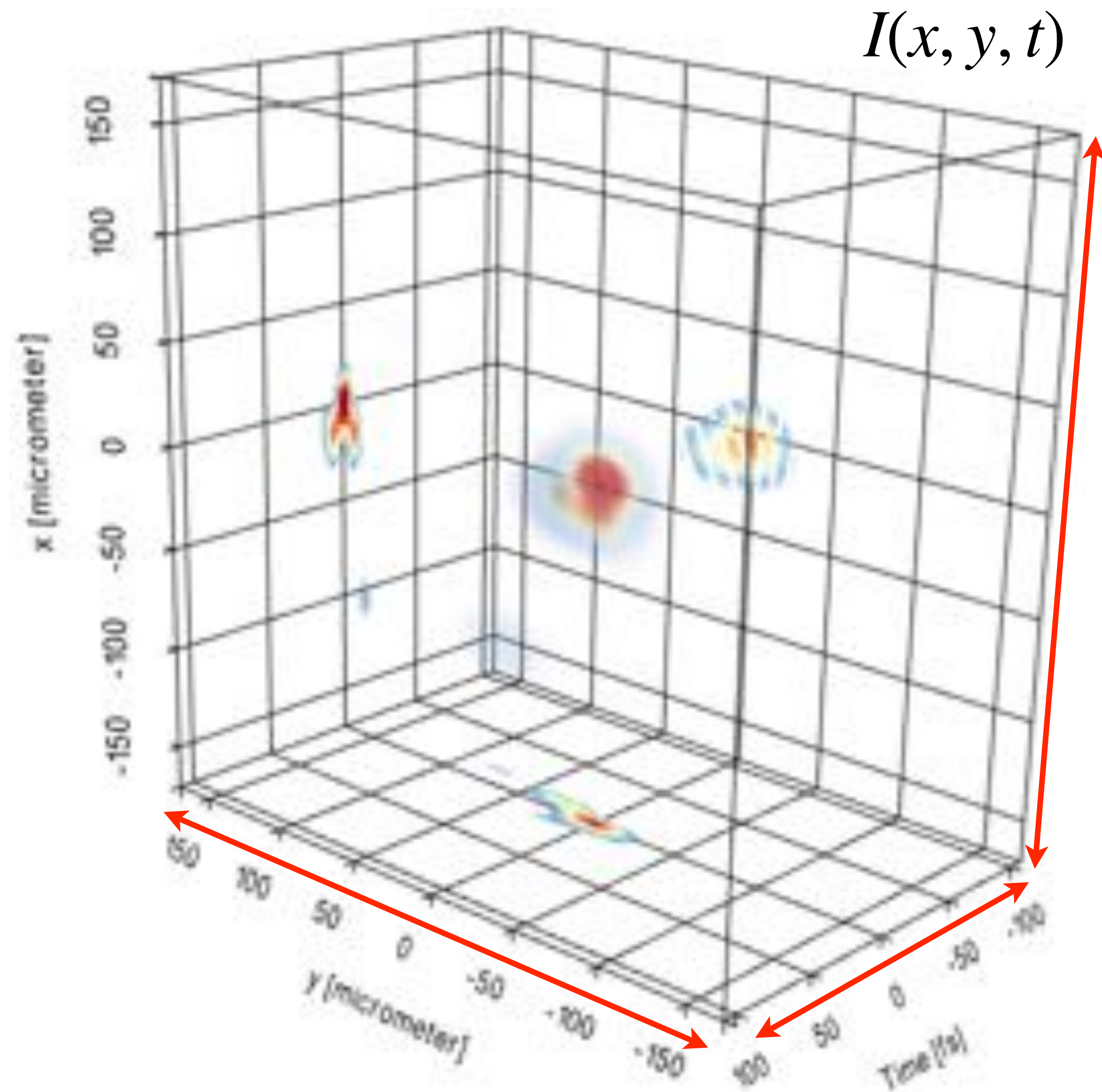
An example

3-D intensity distribution in time

Knowledge necessary for

- Highest peak-intensity
- Accurate simulations
- Spatio-temporal shaping (flying focus etc.)
- ...



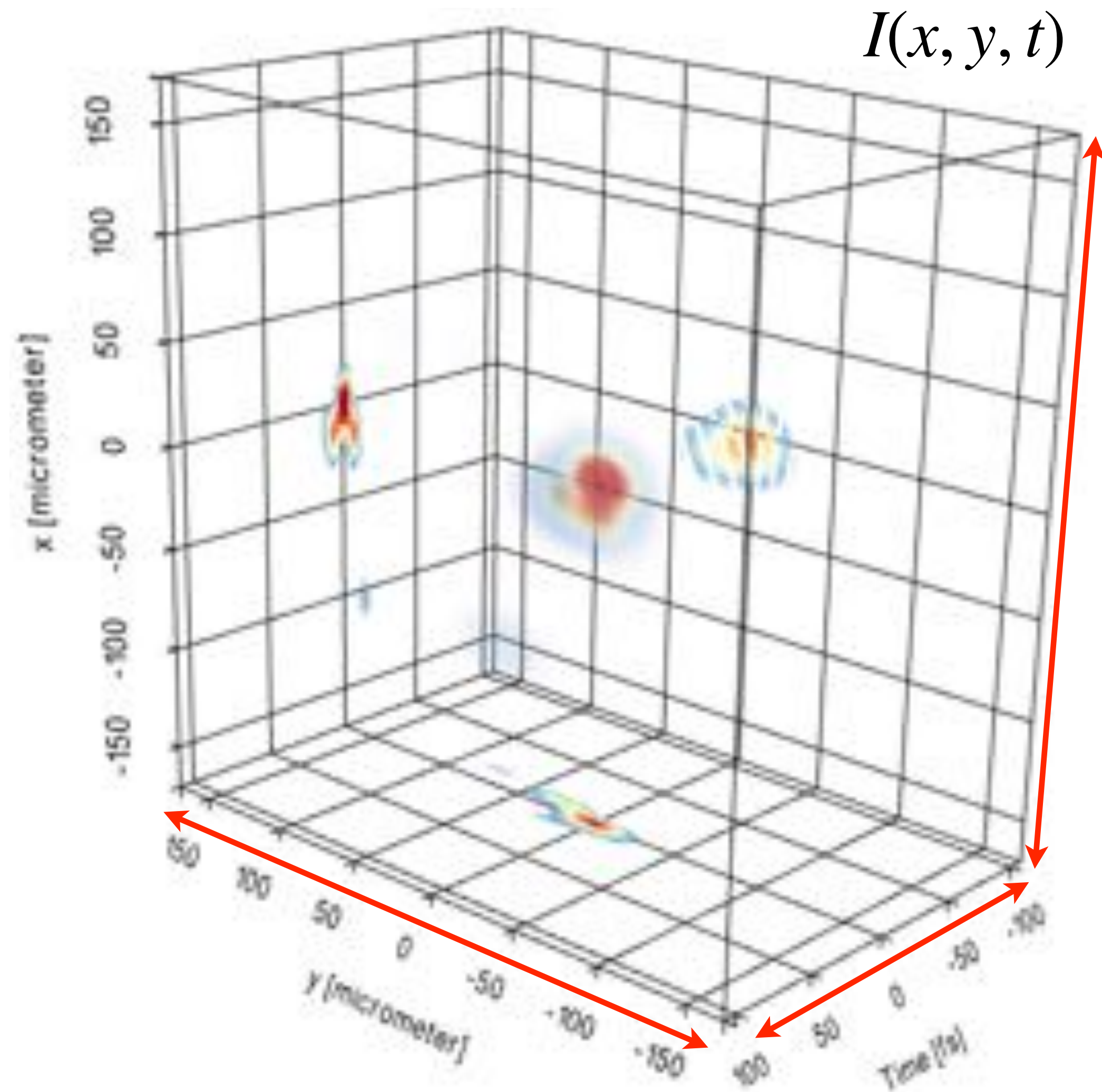


3-D intensity distribution in time

$$n = n_x \times n_y \times n_\lambda \sim 1000 \times 1000 \times 100 = 10^8 \text{ voxels}$$

100 million parameters: Need many measurements

Common solution: Fourier transform spectroscopy (INSIGHT, TERMITES) with >1000 2D measurements at 1 MP



3-D intensity distribution in time

$$n = n_x \times n_y \times n_\lambda \sim 1000 \times 1000 \times 100 = 10^8 \text{ voxels}$$

100 million parameters: Need many measurements

Common solution: Fourier transform spectroscopy (INSIGHT, TERMITES) with >1000 2D measurements at 1 MP

But are voxels really a good base function choice?

Ultra-intense laser characterization

Multi-spectral, modal reconstruction



$$I(x, y, t) = \left\| \mathcal{F} \left[\sqrt{I(x, y, \omega)} \cdot \exp(i\Phi(x, y, \omega)) \right] \right\|^2$$

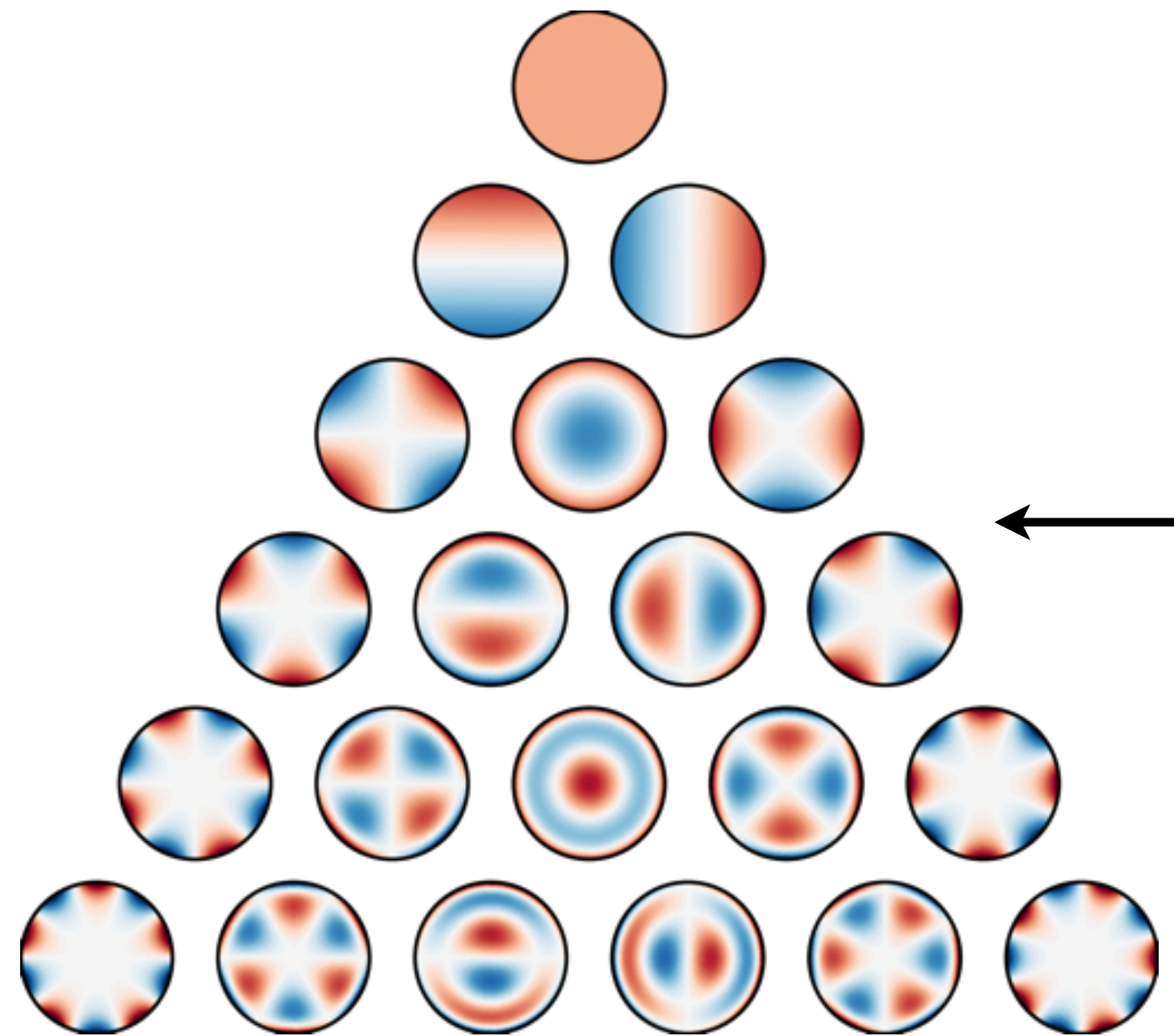


This is the important part,
describing the focused intensity!

Ultra-intense laser characterization

Multi-spectral, modal reconstruction

$$I(x, y, t) = \left\| \mathcal{F} \left[\sqrt{I(x, y, \omega)} \cdot \exp(i\Phi(x, y, \omega)) \right] \right\|^2$$



We know there is a very good base to describe phase:
Zernike polynomials

$$Z_n^m(\rho, \varphi) = R_n^m(\rho) \cos(m \varphi)$$

$$Z_n^{-m}(\rho, \varphi) = R_n^m(\rho) \sin(m \varphi),$$

Ultra-intense laser characterization

Multi-spectral, modal reconstruction



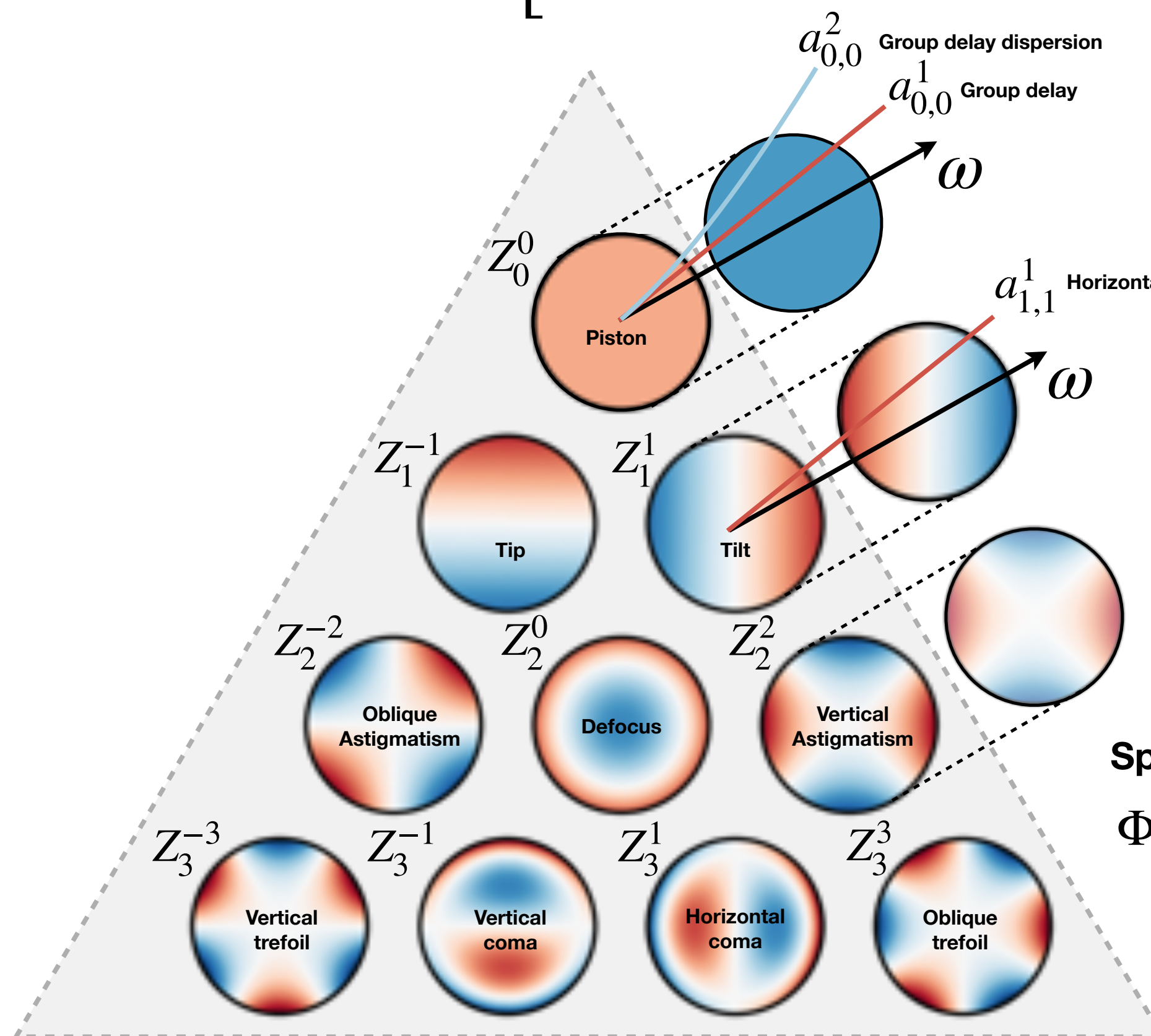
$$I(x, y, t) = \left\| \mathcal{F} \left[\sqrt{I(x, y, \omega)} \cdot \exp(i\Phi(x, y, \omega)) \right] \right\|^2$$

We also know there is a very good way to describe spectral phase: **Taylor expansion** (*group delay, group delay dispersion, etc.*)

Ultra-intense laser characterization

Multi-spectral, modal reconstruction

$$I(x, y, t) = \left\| \mathcal{F} \left[\sqrt{I(x, y, \omega)} \cdot \exp \left(i\Phi(x, y, \omega) \right) \right] \right\|^2$$



Can describe the **hyperspectral wavefront** using **Zernike-modes** and **Taylor-expansion** in frequency

Spatio-spectral phase

$$\Phi(x, y, \omega) = \sum_{m,n,i} a_{m,n}^i (\omega - \omega_0)^i Z_n^m(x, y)$$

Spatial phase $\varphi(x, y) = \sum_{m,n} a_{m,n} Z_n^m(x, y).$

Ultra-intense laser characterization

Multi-spectral, modal reconstruction



$$I(x, y, t) = \left\| \mathcal{F} \left[\sqrt{I(x, y, \omega)} \cdot \exp \left(i\Phi(x, y, \omega) \right) \right] \right\|^2$$

$$\Phi(x, y, \omega) = \sum_{m,n,i} a_{m,n}^i (\omega - \omega_0)^i Z_n^m(x, y)$$

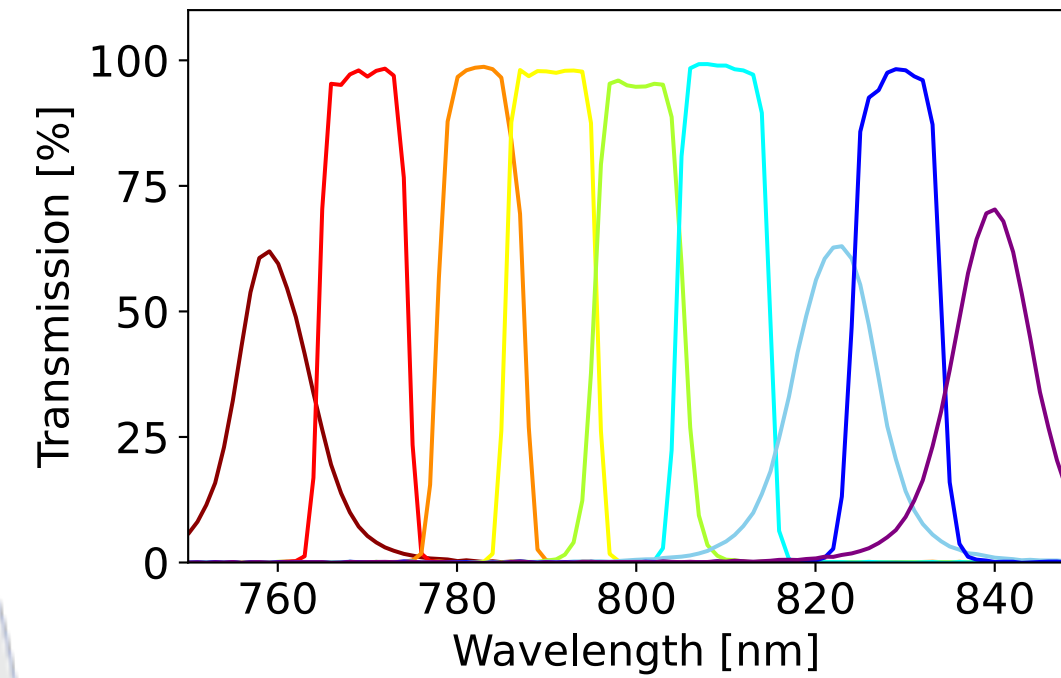
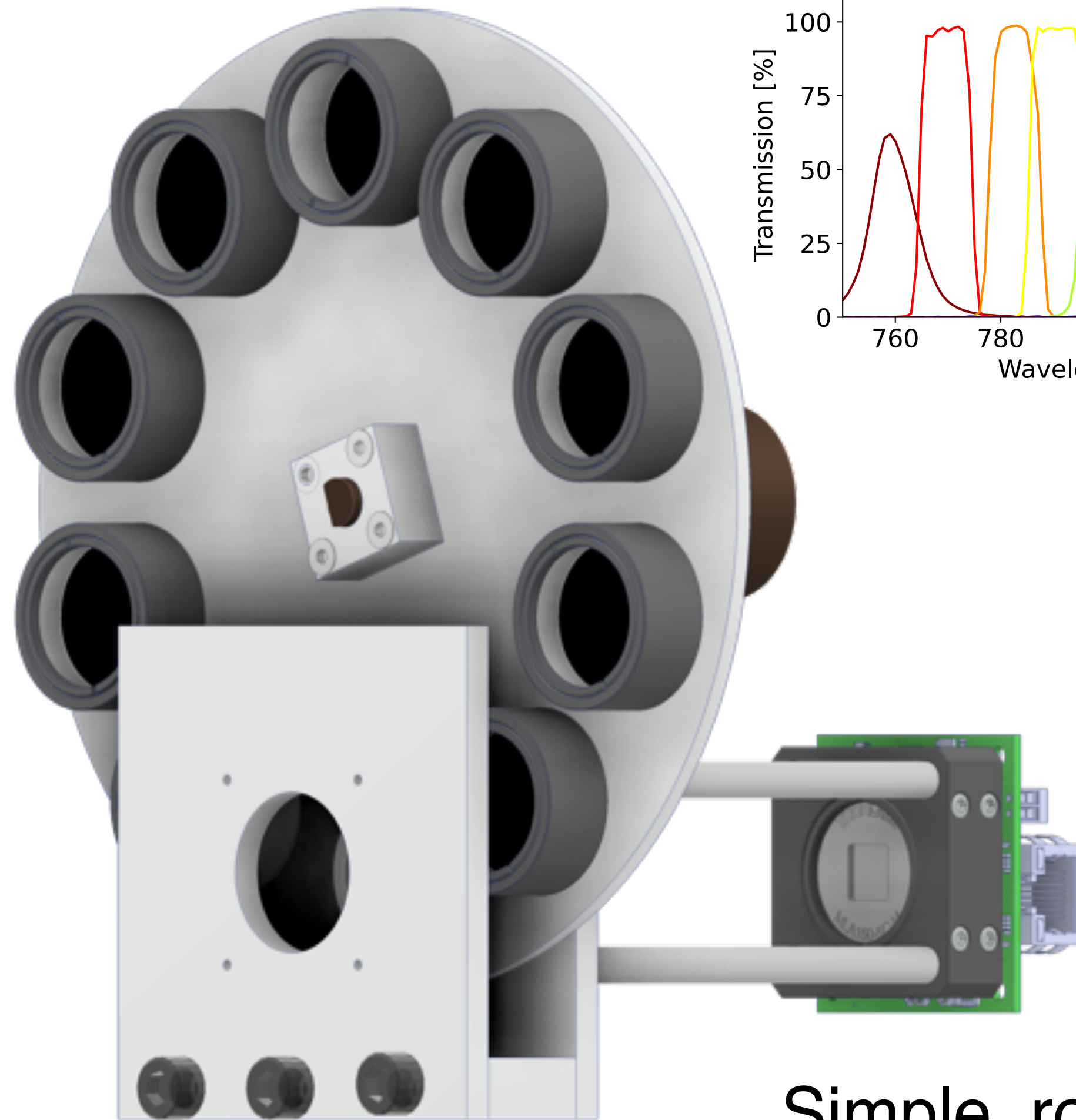
Can describe the **hyperspectral wavefront** using **Zernike-modes and Taylor-expansion in frequency**

Instead of $> 1,000,000$ voxels we only need to *reconstruct dominant mode coefficients*

Allows us to retrieve spatio-temporal couplings within a few measurements

Ultra-intense laser characterization

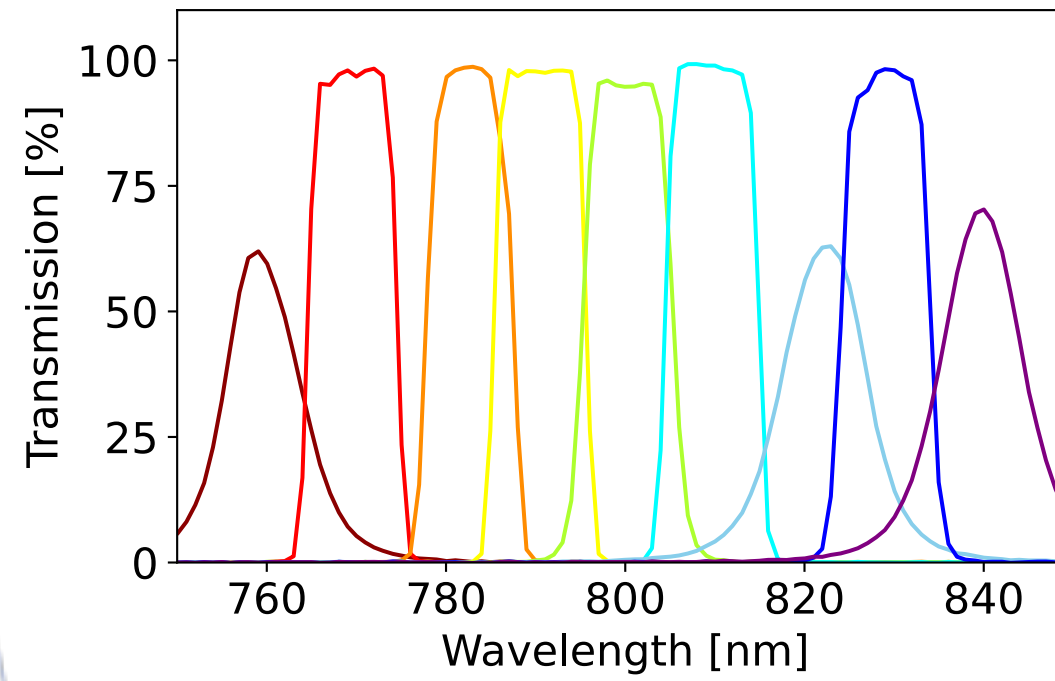
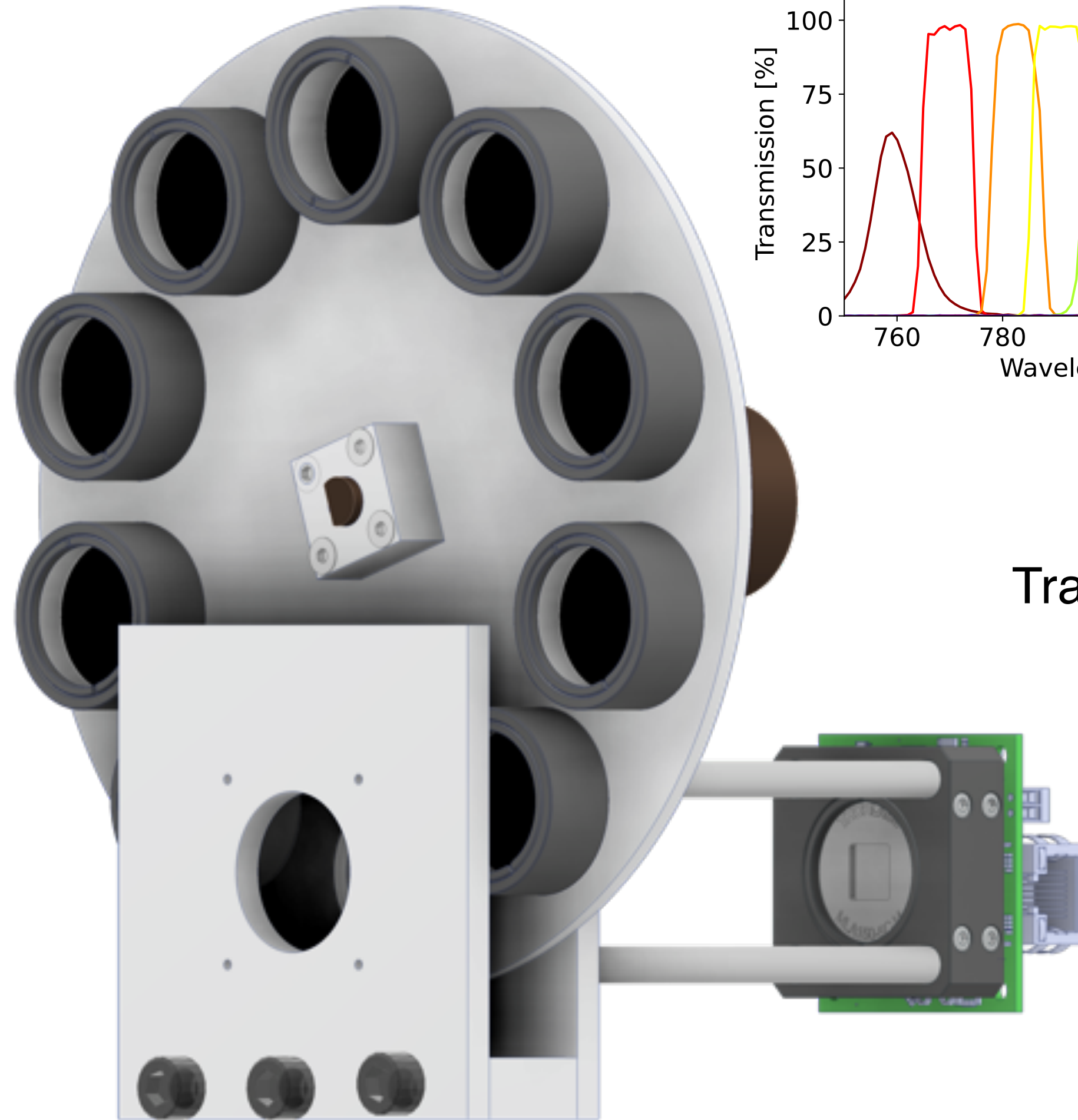
FALCON - Fast Acquisition of Laser Couplings using Narrowband Filters



Simple, robust device

Ultra-intense laser characterization

FALCON - Fast Acquisition of Laser Couplings using Narrowband Filters



This is for a simple 2x2 lenslet SH detector

$$\begin{pmatrix} s_{x,\omega_1}(0,0) \\ s_{x,\omega_1}(0,1) \\ s_{x,\omega_1}(1,0) \\ s_{x,\omega_1}(1,1) \\ s_{y,\omega_1}(0,0) \\ s_{y,\omega_1}(0,1) \\ s_{y,\omega_1}(1,0) \\ s_{y,\omega_1}(1,1) \\ s_{x,\omega_2}(0,0) \\ s_{x,\omega_2}(0,1) \\ s_{x,\omega_2}(1,0) \\ s_{x,\omega_2}(1,1) \\ s_{y,\omega_2}(0,0) \\ s_{y,\omega_2}(0,1) \\ s_{y,\omega_2}(1,0) \\ s_{y,\omega_2}(1,1) \end{pmatrix} = \begin{pmatrix} \frac{dZ_1^{-1}}{dx} & \frac{dZ_1^1}{dx} & \frac{dZ_0^0}{dx} & \tilde{\omega}_1 & \frac{dZ_1^{-1}}{dx} & \tilde{\omega}_1 & \frac{dZ_1^1}{dx} & \tilde{\omega}_1 \\ \frac{dZ_1^{-1}}{dx} & \frac{dZ_1^1}{dx} & \frac{dZ_0^0}{dx} & \tilde{\omega}_1 & \frac{dZ_1^{-1}}{dx} & \tilde{\omega}_1 & \frac{dZ_1^1}{dx} & \tilde{\omega}_1 \\ \frac{dZ_1^{-1}}{dx} & \frac{dZ_1^1}{dx} & \frac{dZ_0^0}{dx} & \tilde{\omega}_1 & \frac{dZ_1^{-1}}{dx} & \tilde{\omega}_1 & \frac{dZ_1^1}{dx} & \tilde{\omega}_1 \\ \frac{dZ_1^{-1}}{dx} & \frac{dZ_1^1}{dx} & \frac{dZ_0^0}{dx} & \tilde{\omega}_1 & \frac{dZ_1^{-1}}{dx} & \tilde{\omega}_1 & \frac{dZ_1^1}{dx} & \tilde{\omega}_1 \\ \frac{dZ_1^{-1}}{dy} & \frac{dZ_1^1}{dy} & \frac{dZ_2^{-2}}{dy} & \tilde{\omega}_1 & \frac{dZ_1^{-1}}{dy} & \tilde{\omega}_1 & \frac{dZ_2^2}{dy} & \tilde{\omega}_1 \\ \frac{dZ_1^{-1}}{dy} & \frac{dZ_1^1}{dy} & \frac{dZ_2^{-2}}{dy} & \tilde{\omega}_1 & \frac{dZ_1^{-1}}{dy} & \tilde{\omega}_1 & \frac{dZ_2^2}{dy} & \tilde{\omega}_1 \\ \frac{dZ_1^{-1}}{dy} & \frac{dZ_1^1}{dy} & \frac{dZ_2^{-2}}{dy} & \tilde{\omega}_1 & \frac{dZ_1^{-1}}{dy} & \tilde{\omega}_1 & \frac{dZ_2^2}{dy} & \tilde{\omega}_1 \\ \frac{dZ_1^{-1}}{dy} & \frac{dZ_1^1}{dy} & \frac{dZ_2^{-2}}{dy} & \tilde{\omega}_1 & \frac{dZ_1^{-1}}{dy} & \tilde{\omega}_1 & \frac{dZ_2^2}{dy} & \tilde{\omega}_1 \\ \frac{dZ_1^{-1}}{dx} & \frac{dZ_1^1}{dx} & \frac{dZ_0^0}{dx} & \tilde{\omega}_2 & \frac{dZ_1^{-1}}{dx} & \tilde{\omega}_2 & \frac{dZ_1^1}{dx} & \tilde{\omega}_2 \\ \frac{dZ_1^{-1}}{dx} & \frac{dZ_1^1}{dx} & \frac{dZ_0^0}{dx} & \tilde{\omega}_2 & \frac{dZ_1^{-1}}{dx} & \tilde{\omega}_2 & \frac{dZ_1^1}{dx} & \tilde{\omega}_2 \\ \frac{dZ_1^{-1}}{dx} & \frac{dZ_1^1}{dx} & \frac{dZ_0^0}{dx} & \tilde{\omega}_2 & \frac{dZ_1^{-1}}{dx} & \tilde{\omega}_2 & \frac{dZ_1^1}{dx} & \tilde{\omega}_2 \\ \frac{dZ_1^{-1}}{dx} & \frac{dZ_1^1}{dx} & \frac{dZ_0^0}{dx} & \tilde{\omega}_2 & \frac{dZ_1^{-1}}{dx} & \tilde{\omega}_2 & \frac{dZ_1^1}{dx} & \tilde{\omega}_2 \\ \frac{dZ_1^{-1}}{dy} & \frac{dZ_1^1}{dy} & \frac{dZ_2^{-2}}{dy} & \tilde{\omega}_2 & \frac{dZ_1^{-1}}{dy} & \tilde{\omega}_2 & \frac{dZ_2^2}{dy} & \tilde{\omega}_2 \\ \frac{dZ_1^{-1}}{dy} & \frac{dZ_1^1}{dy} & \frac{dZ_2^{-2}}{dy} & \tilde{\omega}_2 & \frac{dZ_1^{-1}}{dy} & \tilde{\omega}_2 & \frac{dZ_2^2}{dy} & \tilde{\omega}_2 \\ \frac{dZ_1^{-1}}{dy} & \frac{dZ_1^1}{dy} & \frac{dZ_2^{-2}}{dy} & \tilde{\omega}_2 & \frac{dZ_1^{-1}}{dy} & \tilde{\omega}_2 & \frac{dZ_2^2}{dy} & \tilde{\omega}_2 \\ \frac{dZ_1^{-1}}{dy} & \frac{dZ_1^1}{dy} & \frac{dZ_2^{-2}}{dy} & \tilde{\omega}_2 & \frac{dZ_1^{-1}}{dy} & \tilde{\omega}_2 & \frac{dZ_2^2}{dy} & \tilde{\omega}_2 \end{pmatrix} \begin{pmatrix} a_{0,0}^0 \\ a_{1,-1}^0 \\ a_{1,1}^0 \\ a_{0,0}^1 \\ a_{1,-1}^1 \\ a_{1,1}^1 \end{pmatrix}$$

Translate into an inverse problem

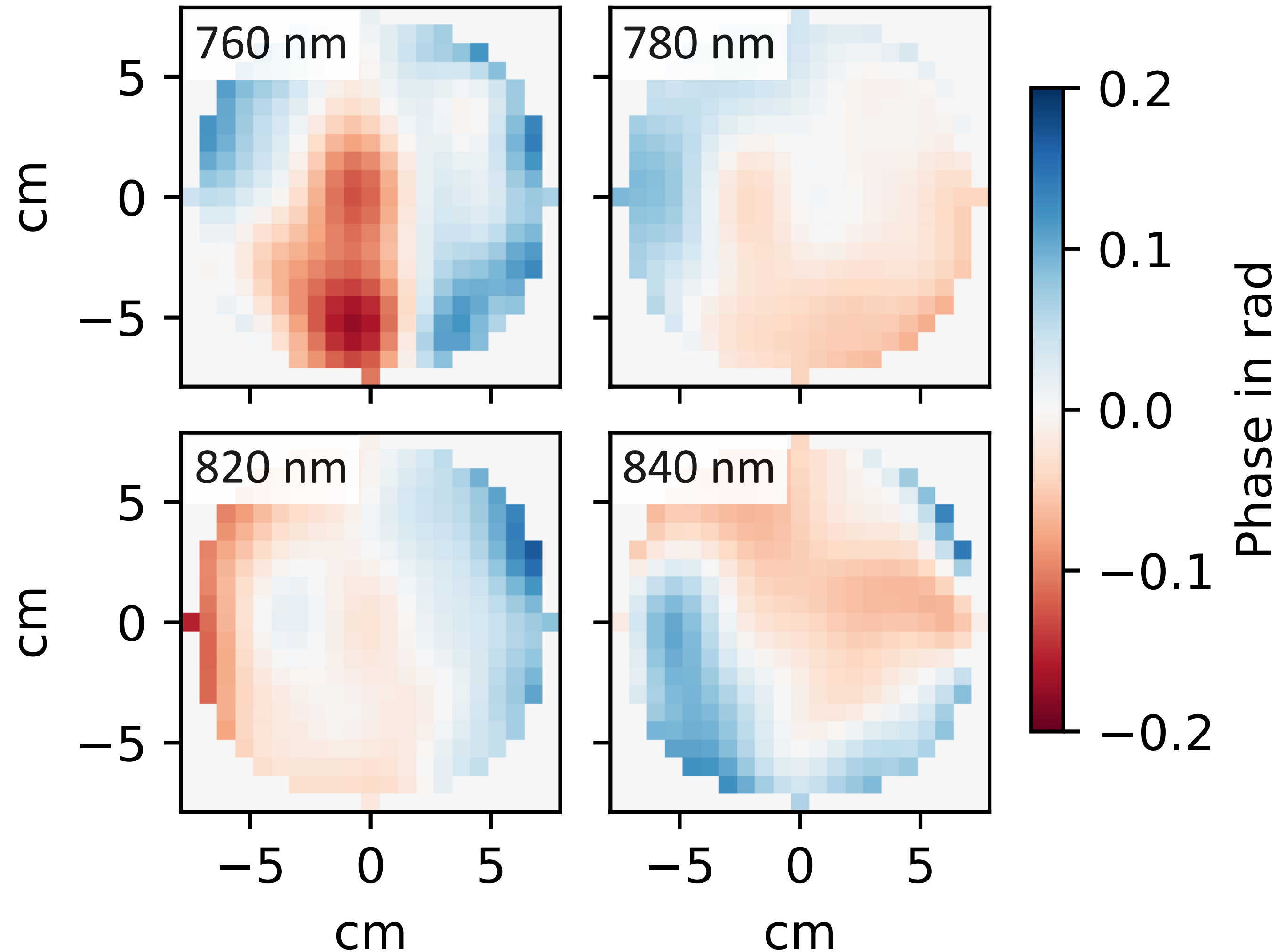
• N. Weiße, J. Esslinger et al. Measuring spatial-temporal couplings using modal multi-spectral wavefront reconstruction, Opt. Express 31, 19733-19745 (2023)

Ultra-intense laser characterization

Measurement of STCs of the ATLAS petawatt laser



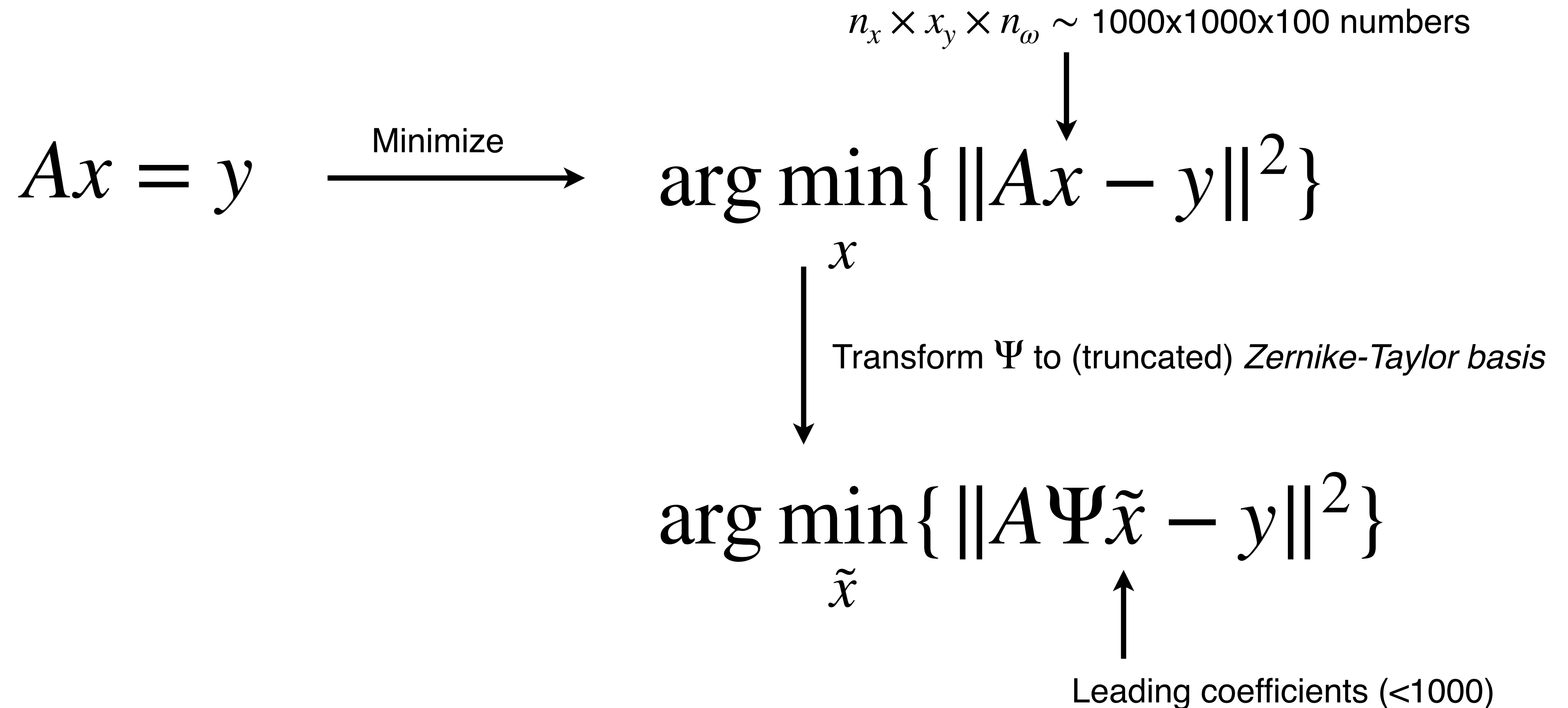
- Full measurement takes ~ 1 minute
(9 wavelengths, 5 shots each)
- Measurement shows couplings in ATLAS are $< \lambda/10$ between 780 - 820 nm
- FALCON measurement now routinely performed every day after focus measurements



• *N. Weiße, J. Esslinger et al. Measuring spatial-temporal couplings using modal multi-spectral wavefront reconstruction, Opt. Express 31, 19733-19745 (2023)*

Ultra-intense laser characterization

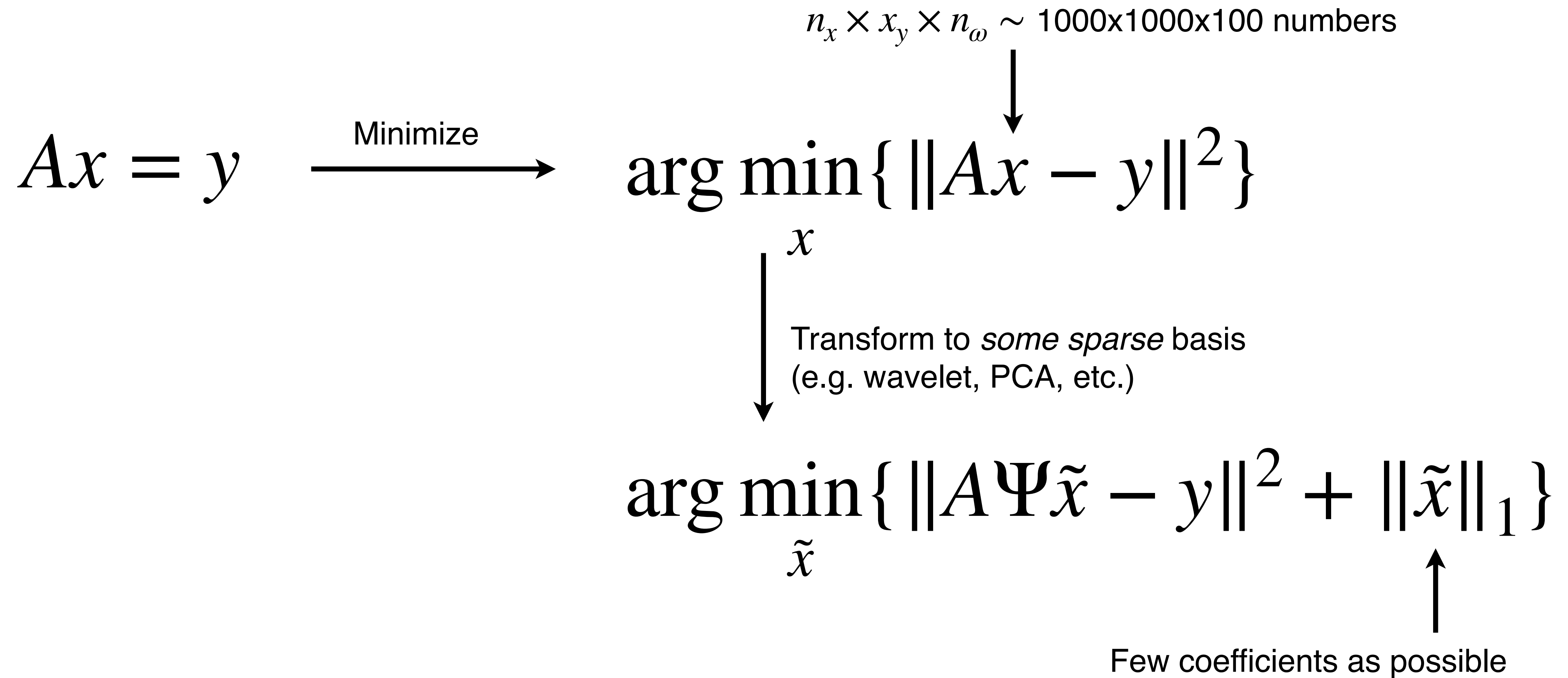
Least-squares in Zernike-Taylor basis



Much more robust reconstruction!

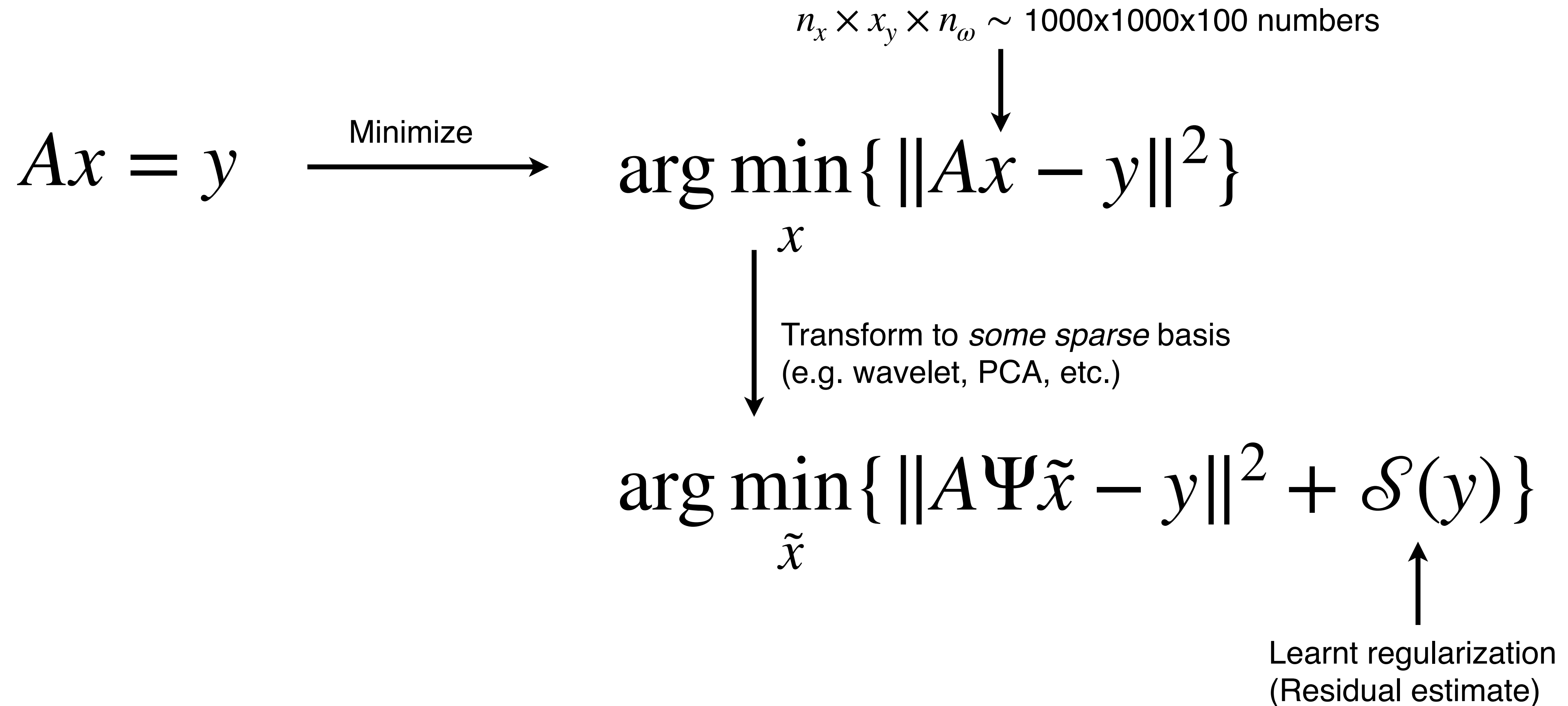
Ultra-intense laser characterization

Compressed sensing



Ultra-intense laser characterization

Deep compressed sensing

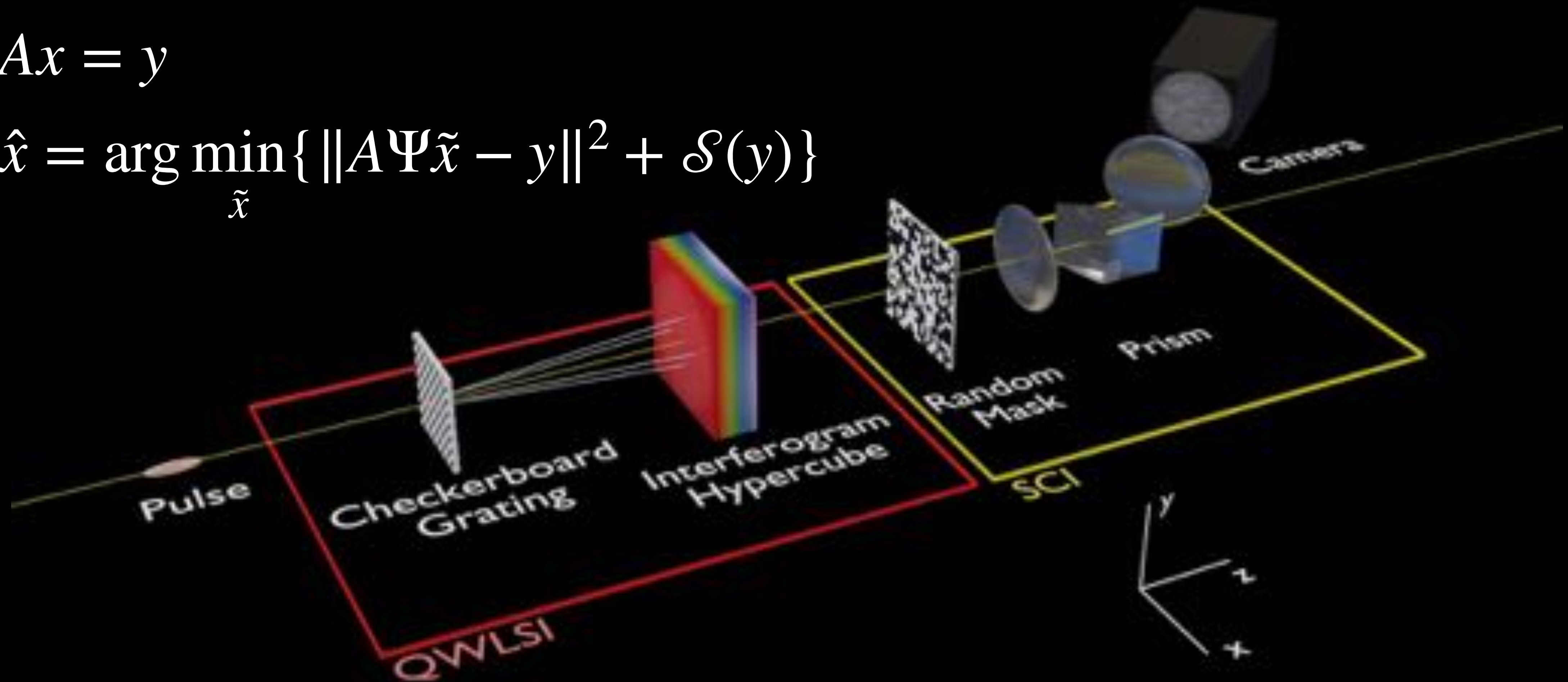


Ultra-intense laser characterization

Deep compressed sensing

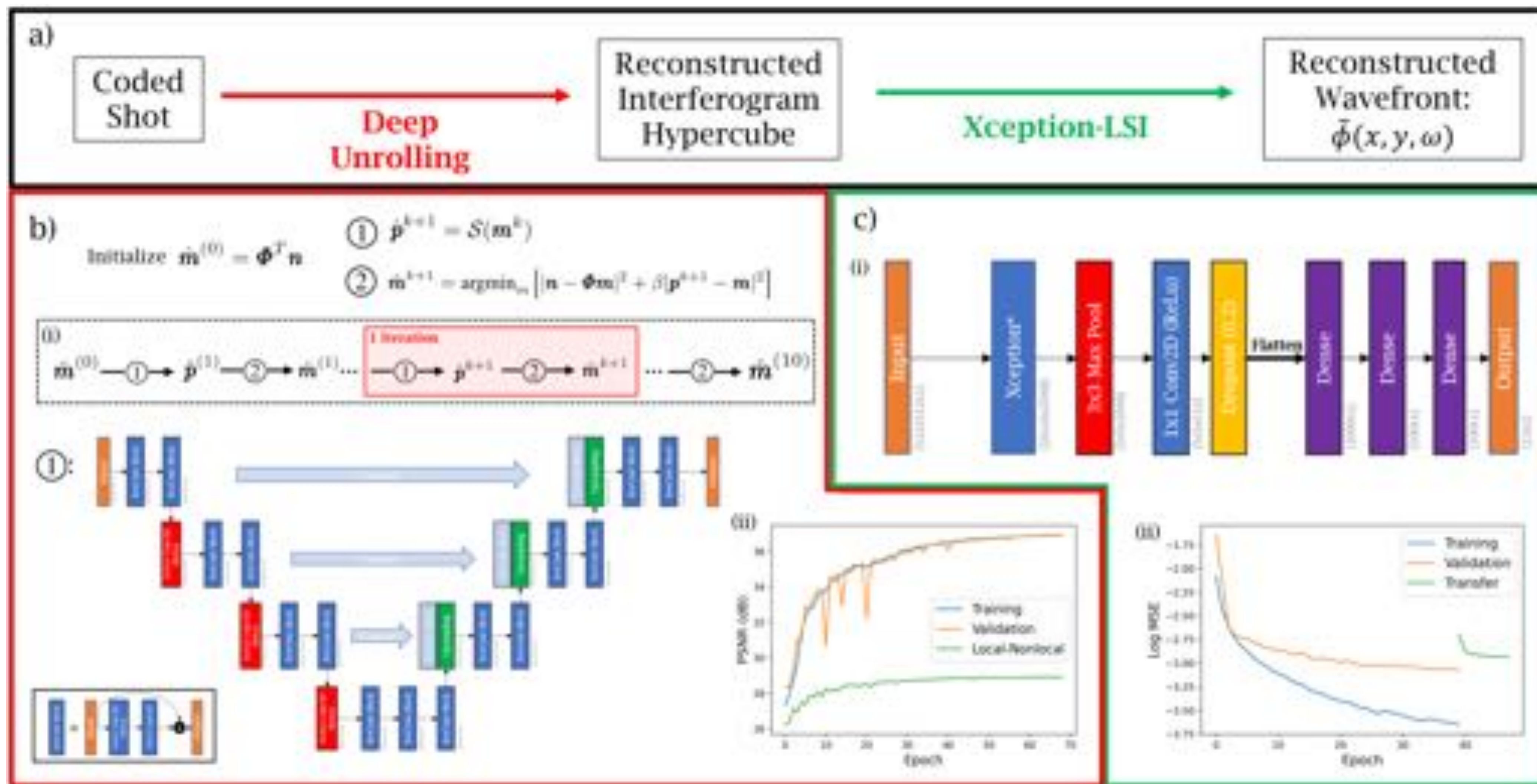
$$Ax = y$$

$$\hat{x} = \arg \min_{\tilde{x}} \{ \|A\Psi\tilde{x} - y\|^2 + \mathcal{S}(y) \}$$



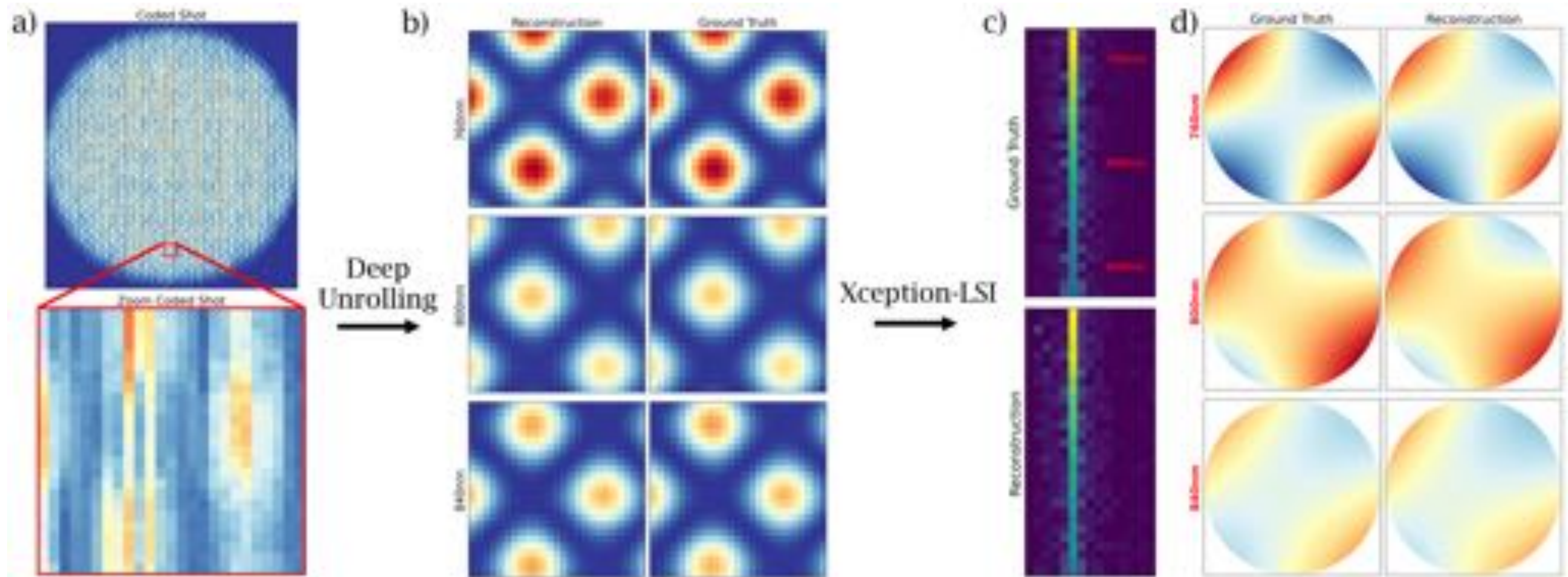
Ultra-intense laser characterization

Deep compressed algorithm unrolling



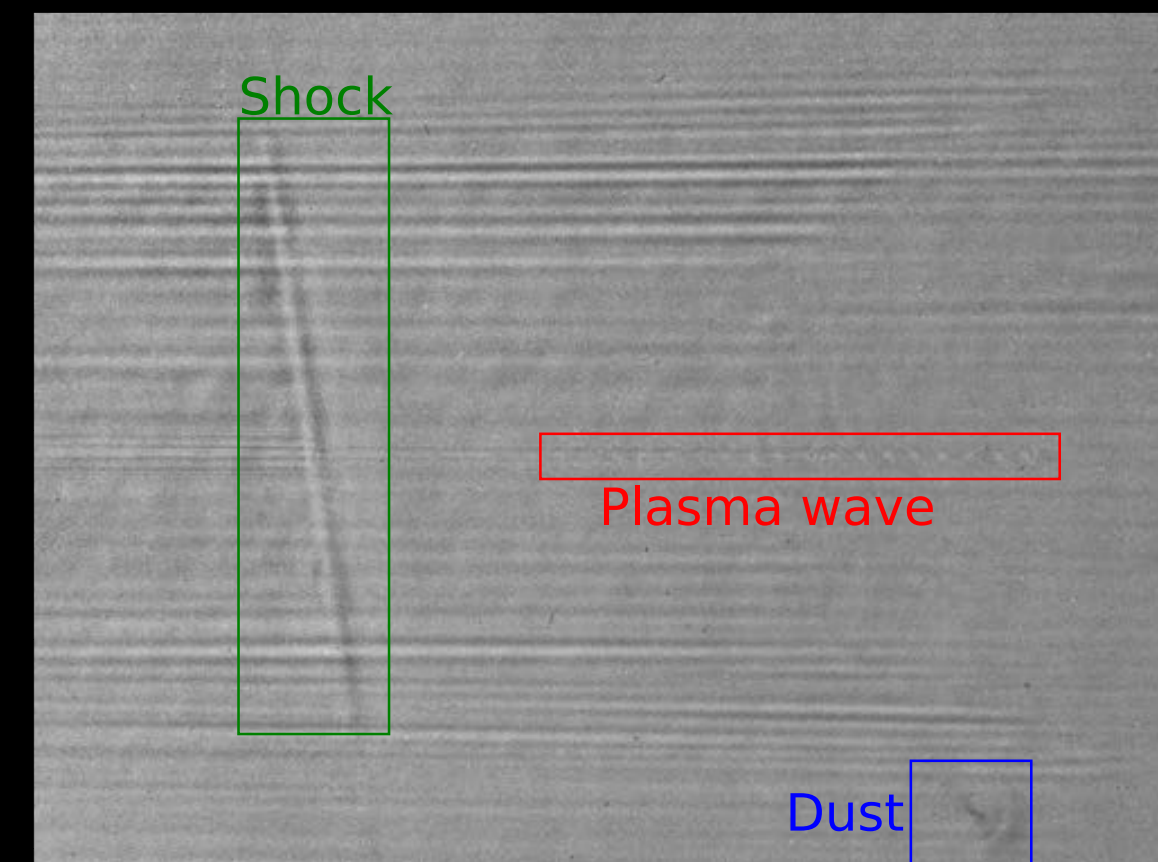
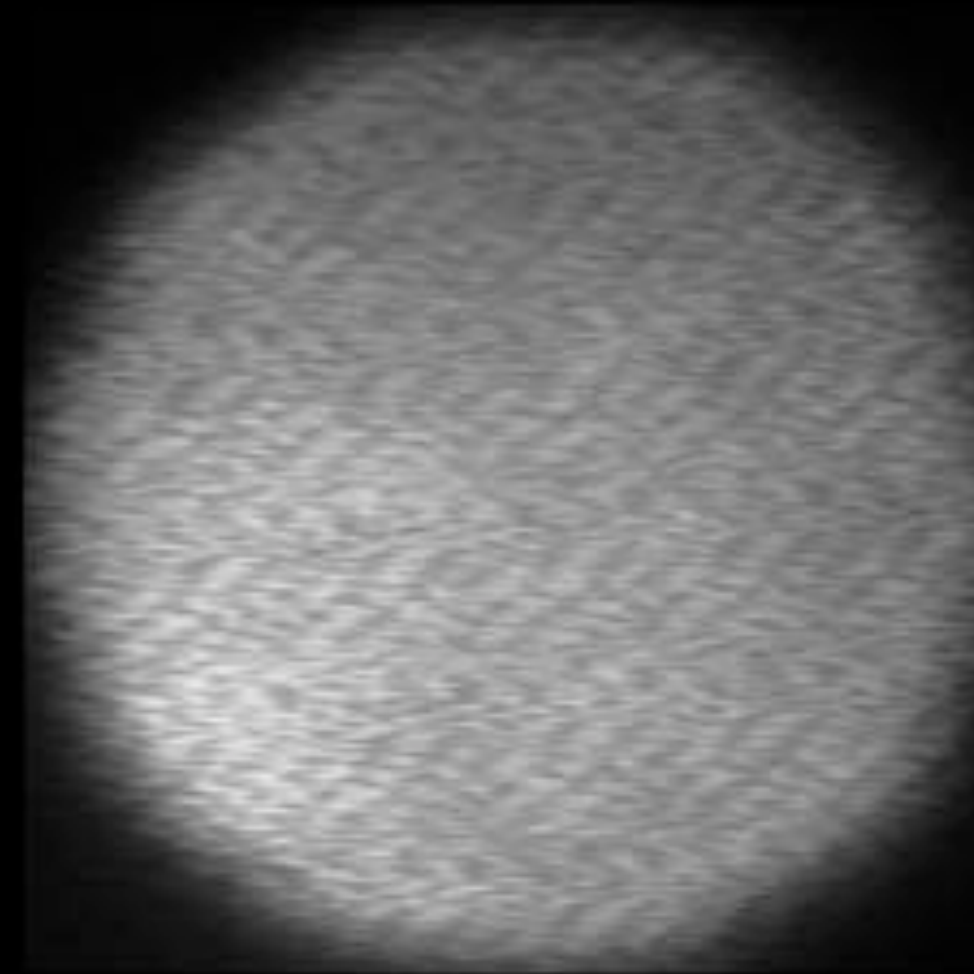
Ultra-intense laser characterization

Deep compressed algorithm unrolling



Conclusions and Outlook

- Machine learning is quickly advancing in laser-plasma physics community
- Physics-driven developments can improve essential building blocks of machine-learning
- Presented new Bayesian optimization approaches using multiple objectives and fidelities
- Presented new approaches to measuring spatio-temporal couplings; single-shot diagnostic under development
- Many other applications in development, e.g. object detection, etc.



Thank you for your attention!

Dr. Andreas Döpp
Am Coulombwall 1 · 85748 Garching · Germany
a.doepp@lmu.de · www.pulse.physik.lmu.de

